LaserGauge: Development of a device for automatic measurement of drilled bore depth in bone during surgery

by

Daniel Demsey

A THESIS SUBMITTED IN PARTIAL FULFILLMENT OF

THE REQUIREMENTS FOR THE DEGREE OF

MASTER OF APPLIED SCIENCE

in

The Faculty of Graduate and Postdoctoral Studies

(Biomedical Engineering)

THE UNIVERSITY OF BRITISH COLUMBIA

(Vancouver)

July 2017

Abstract

Purpose: This thesis comprised two main phases. Initial work focused on clarifying the need and use case for a novel device to measure drilled bore depth in bone during osteosynthesis surgery. Next, I demonstrated the feasibility and reliability of an optical sensing device for automatic measurement of drilled bore depth in bone during surgery compared with conventional methods.

Methods: I completed a structured Needs Assessment followed by an Engineering Design process to develop a series of prototypes using laser displacement sensors mounted on a surgical drill to determine drilled bore depth in bone. In all versions of the prototypes bore depth was computed based on a characteristic pattern of drilling velocity in bicortical bone. Prototypes consisted of one or more laser displacement sensors sending displacement and time data to a microprocessor and then a personal computer. After data filtering with a second order Butterworth filter velocity and acceleration were calculated using differentiation and double differentiation. Characteristic spikes in velocity and acceleration indicated cortical breach and allowed identification of bore depth. Exploratory experiments were done with multiple sensor arrangement concepts in porcine long bones, and more rigorous final evaluation experiments were done with the lead designs in pig hind limbs with comparison to CT scan as 'gold standard'.

Results: In exploratory experiments a design involving two laser displacement sensors angled towards the drilling axis measuring distance from a mock drill guide performed better than alternative designs. This design in final evaluation experiments showed superior performance to the conventional depth gauge under three clinically relevant drilling conditions (standard

deviation 0.70 mm vs. 1.38 mm, 0.86 mm vs. 3.79 mm, 0.80 mm vs. 3.19 mm). A positive bias was present in all drilling conditions.

Conclusions: An optical sensing device can be used to measure bore depth in bone during surgery.

Lay Summary

This thesis describes the development of a new instrument for use in surgery on the bony skeleton. The purpose of the instrument is to measure the depth of bore drilled in bone, to allow the surgeon to make appropriate choices on the size of screw or other implant. The device makes use of a laser-based displacement measurement sensor.

Preface

All the work described in this thesis is that of the author, with the exception of that in the section labelled 'Prior Work.' The Needs Assessment, Design, and Experimental sections were carried out by the author. Juan Pablo Gomez Arrunategui, a Master's student from the Surgical Technologies Lab assisted with the experiments and developed the Arduino code and the Matlab code for the data storage. Juan also assisted in in the electrical components of the prototype section.

No part of this thesis has been published at the time of this writing, however a manuscript is in preparation.

Table of Contents

Abstract ii

Lay Summary iv

Preface v

Table of Contents vi

List of Tables ix

List of Figures x

Acknowledgements xii

Dedication xiii

1 Introduction 1

1.1 Overview 1

1.2 Prior Work 4

1.3 Background and Literature Review 5

1.3.1 Bone Drilling in Clinical Practice 5

1.3.2 Bone Anatomy and Screw Placement 7

1.3.3 Alternatives to Surgical Depth Gauge 8

1.3.3 Research on Surgical Bone Drilling 10

1.3.4 Porcine Surgical Modelling 13

1.4 Thesis Overview 14

2 Needs Assessment 15

2.1 Overview 15

2.2 Prior Work 15

2.3 Needs Assessment 16

2.3.1 Interviews with Practicing Surgeons 16

2.3.2 OR Observations 17

2.3.4 Updated Needs Statement 18

2.4 Context Identification 19

2.4.1 Clinical Uses of the Depth Gauge 19

2.4.2 Surgical Drills 20

2.4.3 Surgical Screws 23

2.4.4 Surgical Exposure Dimensional Analysis 25

2.4.5 Fixation Construct Analysis 28

2.4.6 Current Surgical Depth Gauge 31

2.5 Problem Statement 31

3 Design 33

3.1 Overview 33

3.2 Problem Statement 33

3.3 Concept 33

3.4 Design Specifications 35

3.5 Functional Structural Decomposition 36

3.6 Sensor 37

3.6.1 Concept Selection 37
3.6.2 Optical Sensing 37
3.6.3 Laser Triangulation 38
3.6.4 Sensor Orientation 39
3.7 Microprocessor 41
3.8 Algorithm 41
3.9 User Interface 42
3.10 Mounting Assembly 42
3.11 Power Supply 42
3.12 Housing 43
3.13 Prototyping 43
3.13.1 Single sensor, parallel to drilling axis, measuring from tissue 43
3.13.2 Dual sensor, parallel to drilling axis, measuring from tissue 46
3.13.3 Dual sensor, angled towards drill bit, measuring from tissue 47
3.13.4 Dual sensor, angled towards drill bit, measuring from drill guide 48
3.14 ENG PHYS Design Project 49
3.15 Design Summary 50

4 Materials and Methods 51
4.1 Overview 51
4.2 Animal Models 51
4.2.1 Chicken Long Bone 51
4.2.2 Porcine Long Bone 51
4.2.3 Porcine Hind Limb 52
4.3 Exploratory Experiments 53
4.4 Evaluation of Final Concept 55

5 Results 59
5.1 Overview 59
5.2 Final Evaluation Results 59

6 Discussion 64
6.1 Significance of Design 64
6.2 Sensor Concepts 64
6.2.1 Single vs. Dual Sensors 64
6.2.2 Parallel vs. Angled Sensors 67
6.2.3 Tissue vs. Drill Guide Reference 68
6.3 Drilling Conditions 69
6.3.1 Condition SD 69
6.3.2 Condition AD 69
6.3.3 Condition SM 70
6.4 Final Concept Selection 70
6.5 Bore Depth 'Gold Standard' 70
6.5.1 Bone Geometry 70
6.5.2 Measurement Methods 71
6.5.3 Interpretation of Measurement by Surgeon 72
6.5.4 Required Precision 72
6.6 Additional Considerations 73
6.7 Existing Literature 73

6.8 Limitations **73**

7 Conclusion **75**

7.1 Future Work **75**

References **77**

Appendix A – Incision Dimensional Analysis **80**

A.1 Overview **80**

A.2 Data Tables **80**

Appendix B – Fixation Construct Analysis **82**

Appendix C – Exploratory Experiments **83**

C.1 Overview **83**

C.2 Single parallel sensor measuring from tissue **83**

C.3 Paired parallel sensors measuring from tissue **85**

C.4 Paired angled sensors measuring from tissue **86**

C.5 Paired angled sensors measuring from drill guide **87**

Appendix D – Final Evaluation Experiments **88**

Appendix E – Sterilization Approval Process **89**

E.1 Overview **89**

E.2 Approval Process **89**

E.3 Sterilization Methods **89**

E.3.1 Autoclave Steam Sterilization 89

E.3.2 Ethylene Oxide (ETO) Sterilization 90

E.3.3 Chlorine Dioxide (CD) Gas Sterilization 90

E.3.4 Vaporized Hydrogen Peroxide (VHP) Sterilization 91

E.3.5 Hydrogen Peroxide Plasma Sterilization 91

E.3.6 Gamma Ray Sterilization 91

E.3.7 Electron Beam Sterilization 92

List of Tables

Table 1 – Dimensional Analysis Summary 27
Table 2 – Summary of common optical distance sensing method properties 38
Table 3 – Laser displacement sensors available from KEYENCE 39
Table 4 – Results from exploratory experiments 54
Table 5– Final evaluation data summary 60
Table 6 – Mean error and SD for the dual laser prototype compared with conventional depth. 61

List of Figures

Figure 1 - Intellisense Drill (McGinley Orthopedics, USA). An advanced surgical drill with integrated sensors including bore depth measurement 2
Figure 2 - The conventional depth gauge 6
Figure 3 - Long bone anatomy 7
Figure 4 - SMARTdrill (SMD Inc., USA) 9
Figure 5– Typical orthopedic surgical exposure with plates and screws in situ 18
Figure 6 – Distribution of surgical cases using the depth gauge between different services at VGH 20
Figure 7 – Pistol type drill 21
Figure 8 – Pencil type drill 21
Figure 9 – Small Bone Drill Market USA 2015 22
Figure 10 – Medium Bone Drill Market USA 2015 22
Figure 11 – Mandible Screws from Stryker 23
Figure 12 – Upper Face Screws from Stryker 24
Figure 13 - Orthopedic trauma screws from Stryker 24
Figure 14 – Surgical exposure dimensional analysis. Incision dimensions are indicated in green, and bone exposure dimensions are indicated in purple. 26
Figure 15 - Example of incision marking image 27
Figure 16 – Plot of the Incision Dimensional Analysis 28
Figure 17 - Condition SD (straight diaphysis), perpendicular drilling to long axis in diaphyseal bone. Perpendicular entry and exit of screw relative to bone surface. 29
Figure 18 - Condition AD (angled diaphysis), angled drilling to long axis in diaphyseal bone. Angled entry and exit of screw relative to bone surface 29
Figure 19 - Condition SM (straight metaphysis), perpendicular drilling to long axis in metaphyseal bone, angled entry and exit relative to bone surface 30
Figure 20 - Condition AM (angled metaphysis), angled drilling to long axis in metaphyseal bone, perpendicular entry and angled exit relative to bone surface 30
Figure 21 - Screw conditions in Construct Analysis 31
Figure 22 - Relationship between displacement measured and bore depth 34
Figure 23 - Graph of measured displacement and computed velocity, acceleration during bore drilling 35
Figure 24 – Device architecture diagram 37
Figure 25 - Displacement sensor collinear with drilling axis, measuring from tissue surface 40
Figure 26 - Displacement sensor angled relative to drilling axis, measuring from tissue surface 40
Figure 27 - Displacement sensor, collinear or angled, measuring from fixed surface such as drill guide 41
Figure 28 – Single parallel sensor prototype 44
Figure 29 – Data and software flow chart 45
Figure 30 – Prototype circuit diagram 45
Figure 31 - Periodogram for displacement 46
Figure 33 – Dual parallel sensor prototype 47

Figure 34 – Correction for beam angle....48
Figure 35 – Dual sensor, angled towards drill bit....48
Figure 36 – ENG PHYS student design concept....50
Figure 37 - Porcine femur in drilling test....52
Figure 38 - Porcine hindlimb model....53
Figure 39 – Summary of exploratory experiments....54
Figure 40 - Drilling conditions tested....57
Figure 41 - Cumulative frequency distribution for Condition SD....62
Figure 42 - Cumulative frequency distribution for Condition AD....62
Figure 43 - Cumulative frequency distribution for Condition SM....63
Figure 44 – Bland Altman plots for the LaserGauge and the conventional depth gauge comparing to CT scan as 'gold standard'....63
Figure 45 – Effect of drill tilt on sensor readings....65
Figure 46 – Effect of change of drill trajectory on sensor readings....66
Figure 47 – Rotation and irregular bone surface....66
Figure 48 - Two sensors on opposite sides of drilling axis correct for tilt error....67
Figure 49 – Drill guide constraints....68
Figure 50 - Condition SD....69
Figure 51 - Condition AD....69
Figure 52 - Condition SM....70
Figure 53 – Measurement variations in bone bore, shown in cross section. Three arrows indicated three different measurements of bore depth....71

Acknowledgements

I'd like to acknowledge my supervisors, Dr. Antony Hodgson and Dr. Nick Carr for their guidance and support during my graduate studies. Both were extremely generous with their time and their experience. I'd like to thank Dr. Mu Chiao for sitting on my thesis committee.

For salary support I'd like to thank the University of British Columbia Clinician Investigator Program, and more specifically Dr. Sian Spacey and Tessa Feuchuk. For research funds and freedom from clinical responsibilities I'd like to thank the Division of Plastic Surgery, particularly Dr. Mark Hill and Dr. Alex Seal.

Juan Pablo Gomez Arrunategui was indispensable in helping me with the electrical component of the prototype development and with conducting the experiments. Dr. Pierre Guy provided immense assistance with the Needs Assessment and the Final Evaluation experiments. I'd like to thank Masashi Karasawa for his help with producing concept drawings, and the members of the Surgical Technologies Laboratory for their support and hospitality. For facilities support thanks go to the Centre for Hip Health and Mobility and the University of British Columbia.

Most importantly I'd like to thank my family for their support during completion of my thesis, which turned out to be a more challenging and more rewarding experience than any of us imagined.

Dedication

To Dad.

1 Introduction

1.1 Overview

Surgeons who perform orthopedic, plastic, and oral/maxillofacial surgery routinely need to measure the depth of holes drilled in bone. Measuring the drilled bore depth accurately is necessary to select the appropriate screw to use in osteosynthesis surgery. The current methodology uses an instrument called the 'depth gauge', which consists of a hooked wire and a sliding component marked with graduations. Evidence shows that the current method results in placing screws of incorrect length 9% of the time in fixation of distal radius fractures (Ozer and Toker 2011). Incorrect screw length has significant clinical consequences such as rupture of adjacent tendons (Caruso, Vitali, and del Prete 2015; Maschke et al. 2007). Previous interviews with practicing surgeons have also shown that the instrument is frustrating and time consuming to use. Drill guides and drill bits with graduated aspects have attempted to address this, but are likely to be inaccurate. Advanced surgical drills with bore depth measurement features are under development ("Smart Drill – Prevent Plunge, Measure and Control Depth, Determine Bone Density" 2017), but these methods are not compatible with the existing stock of surgical drills, and thus require a significant additional capital investment. There could also be

significant ongoing costs in the form of specialized consumables (eg, device-specific drill bits).

Figure 1 - Intellisense Drill (McGinley Orthopedics, USA). An advanced surgical drill with integrated sensors including bore depth measurement

My overall research objective is therefore to develop a reliable and inexpensive replacement for the current bore depth measurement method that can be retrofitted to existing surgical drills. The design process I used to achieve this goal involved assessing the use cases for such a measurement device, determining design specifications, extending and modifying an existing design concept, and building and testing several prototypes in increasingly realistic use scenarios.

Previous research work in our lab and elsewhere has introduced sensors into the drilling process to detect progress of the drill bit through tissue layers, typically to identify the point where the drill bit breaks though the far bone cortex (Brett et al. 1995; Taylor et al. 2010; Coulson et al. 2013; Benedetto Allotta, Giacalone, and Rinaldi 1997; B. Allotta et al. 1996; Colla and Allotta 1998; Ong and Bouazza-Marouf 1998; Hsu, Lee, and Lin 2001; Wen-Yo Lee and Shih 2006; W.-Y. Lee, Shih, and Lee 2004; Louredo, Díaz, and Gil 2012; Louredo, Diaz, and Gil 2012).

Measurements of force, torque, and displacement have all been used. Most had the primary purpose of attempting to stop drilling automatically to prevent the drill bit from plunging into adjacent tissues. However, these designs did not explicitly measure the depth of the drilled bore and so could not guide screw selection. Additionally, they relied on sensors and actuators within the drill transmission itself, and thus required a new drilling device. At the time that we began this project, we were unaware of any devices focused on the task of accurately measuring the bore depth, so we initially targeted this functionality.

Previous work in our lab demonstrated that a single sensor design, using a linear potentiometer, could be mounted on an existing drill and provide an accurate measure of drilled bore depth in animal tissue (Cavers et al. 2016). Limitations of this design include use of a mechanical arm that intrudes into the surgical field, leading to challenges in developing a mechanical system that is compatible with multiple models of surgical drill.

Because of the limitations we identified related to the mechanical design I evaluated the possibility of using a laser-ranging device for this purpose. I hypothesized that such a device would simplify the overall device design, avoid mechanical interference with the surgical site, and allow for better compatibility with existing drill models. Relatively recently, we have become aware of two related devices that are similar in concept to what we proposed and investigated here: (1) the AutoGauge – a device invented at the AO Foundation in Switzerland that uses a laser displacement sensor measuring displacement from a modified drill guide to compute bore depth, and (2) a patent application by McGinley on a device using a single sensor to detect the leading edge of an instrument passing through materials of variable properties. While these devices will certainly affect our ability to seek a patent on the system presented in

this thesis, neither of these devices have had their performance reported on in the published literature.

My specific research objectives are therefore to:

1. Perform a systematic needs assessment for a bore depth measurement device based on a laser-sensing principle
2. Develop design specifications for the device
3. Develop multiple concepts for a laser sensor device
4. Perform feasibility testing of device concepts
5. Perform accuracy and reliability testing of leading concepts in surgically relevant simulated scenarios

We used commercially available laser displacement sensors for the concept prototypes. The concepts tested included using single vs. multiple sensors, aligning the sensor with the drill axis or at an angle to it, and measuring the displacement from the tissue vs. an instrument surface.

1.2 Prior Work

Our lab previously developed a prototype that incorporated a mechanical displacement sensor attached to a surgical drill. The breakthrough point was identified by analyzing the depth vs time trajectory and observing the point where the drill rapidly accelerated after breaching the distal cortex. The change in displacement between the initial and exit positions was taken to be the bore depth. Previous investigators found that this system could accurately compute the bore depth in an animal model based on the depth vs time trajectory when compared with digital calipers (mean error 0.5mm, standard deviation 0.5mm)(Cavers et al. 2016). However,

the use of a linear sliding mechanism would complicate use of the device in to the operating room. The arm would need to extend into the surgical incision and make contact with the tissue, increasing the profile of the device and obstructing the surgeon's field of view. Furthermore, the device was initially tested in a limited range of settings with animal bones, so the relevance to surgical applications was insufficiently examined. For these reasons, we decided to explore a laser-based alternative approach and evaluate it in more surgically-relevant scenarios. Before explaining our design process in detail, we begin by reviewing the context of the targeted surgical tasks.

1.3 Background and Literature Review

1.3.1 Bone Drilling in Clinical Practice

Fractures of the human skeleton are common and frequently treated with operative fracture reduction and placement of mechanical hardware (osteosynthesis). This facilitates healing and allows early mobilization. The most common osteosynthesis method involves placing plates and screws into the fracture segments to stabilize them in appropriate alignment. The surgeon must choose screws of appropriate length – too short and there is a theoretical risk of a weak fixation construct ("Oxford Textbook of Trauma and Orthopaedics - Oxford Medicine" 2017); too long and there is risk of damage to tissue structures adjacent to the bone (Caruso, Vitali, and del Prete 2015; Maschke et al. 2007).

A depth gauge is commonly used to measure bore depth in bicortical bone osteosynthesis. This is a thin wire instrument with a hook on one end and measurement gradations along its length. The instrument is placed through the drilled bore, hooked on the

far cortex, and gently retracted. The depth of the bore is measured from the gradations marked on the instrument. Focus sessions and individual interviews we conducted with surgeons who use this instrument identified that it is 'frustrating, time consuming, and inaccurate to use.' Measuring bore depth using the current instrument results in placing screws that are too long 9% of the time in certain operations (Ozer and Toker 2011). Screws that are too long can lead to complications such as tendon rupture, which has been discussed in case reports(Schnur and Chang 2000; Caruso, Vitali, and del Prete 2015).

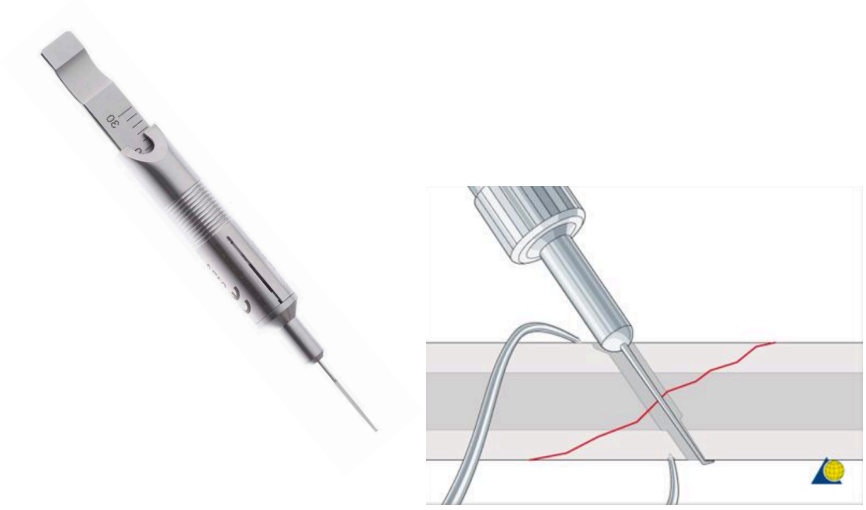

Figure 2 - The conventional depth gauge

Intraoperative fluoroscopy is generally performed to confirm adequate fracture reduction once plates and screws have been placed. Cadaver studies have shown that the standard views obtained will often not show that a screw is the wrong size, as a screw has to be an average of 2.5-6.5mm too long before being identifiable on intra-op X-ray (Maschke et al. 2007). This suggests that many wrong-sized screws go unrecognized. Because incorrect screw sizing is often missed, it is especially important to select the correct screw size initially.

1.3.2 Bone Anatomy and Screw Placement

The long bones of the human skeleton have three sections: the epiphysis, the metaphysis, and the diaphysis (Netter 2014). The main length of the bone shaft is the diaphysis which has outer layer of dense cortical bone. This surrounds the medullary canal, which contains soft bone marrow. The epiphysis at the proximal and distal bone ends consists of a thinner outer layer of cortical bone surrounding a middle section of spongy, cancellous bone. The metaphysis section transitions between the properties of the other two sections. Cortical bone has superior material strength to cancellous bone(Reilly and Burstein 1975; Carter, Schwab, and Spengler 1980). The metaphysis section transitions between the properties of the other two sections.

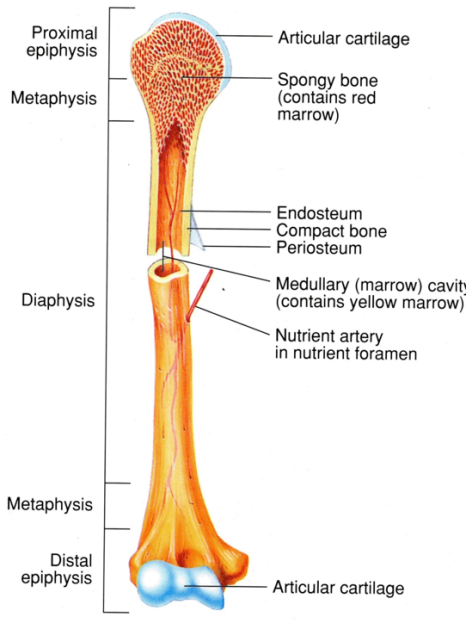

Figure 3 - Long bone anatomy

Screws placed during osteosynthesis surgery should have purchase in the strong cortical portion of the bone ("Oxford Textbook of Trauma and Orthopaedics - Oxford Medicine" 2017).

This means having the screw pass through the cortex on both sides of the bone (bicortical) when putting fixation in the diaphyseal component. The external surface of the metaphysis and epiphysis also has a cortical layer (Rho, Kuhn-Spearing, and Zioupos 1998), and screws placed in these portions of the bone should also engage this cortical layer.

1.3.3 Alternatives to Surgical Depth Gauge

Review of the patents related to the surgical depth gauges found two advanced surgical drills with integrated depth measurement, in addition to other features. Cost information is not publically available for the devices described below but is assumed to be significant. A standard surgical drill costs approximately $20 000 USD.

The Intellisense Drill (McGinley Orthopedics, USA) ("IntelliSense Bone Drill With Auto Depth Measurement and Edge Detection FDA Cleared (VIDEO) |" 2015)includes integrated sensors to determine drilled depth in bone (Figure 1). A combination of a force and displacement sensors are used to measure the drill position and the force of the tissue on the drill, allowing the type of tissue at the drill bit tip to be determined. It also has a programmable 'stop' function to prevent the drill plunging once the bone has been breached. It can be integrated into standard operative techniques, but requires replacement of the existing drill hand piece.

The SMARTdrill (SMD Inc, USA) ("Smart Drill – Prevent Plunge, Measure and Control Depth, Determine Bone Density" 2017) also integrates sensors into a drill hand piece. It uses a combination of force and displacement sensors, and includes a moveable drive assembly in the hand piece to allow mechanical control of drilling depth. Its features include depth

measurement, programmable drilling depth, measurement of bone density, and measurement of drill bit tip performance. It requires replacement of the entire drill hand piece.

Figure 4 - SMARTdrill (SMD Inc., USA)

AO Biomedical Engineering has recently developed an optical sensor based device (the AutoGauge) that attaches to an existing surgical drill, and measurements movement of the drill relative to a custom drill guide. This has been presented at a major orthopedics conference (DKOU 2016). There is currently no published data on the efficacy of this device. My supervisor, Dr. Hodgson and I had a conversation with the lead on this project, Dr. Peter Varga. Dr. Varga shared that his team was working on a concept using optical measurement of drill displacement to compute drilled bore depth in surgical bone drilling. No information on their design has been published in the scientific literature or was available in the patent search process.

1.3.3 Research on Surgical Bone Drilling

Most of the previous research on bone drilling was focused on mathematical modelling of the material properties of the process. The more general case of surgical bone drilling was described using finite element analysis by (Basiaga, Paszenda, and Szewczenko 2010). Qi et al compared rigid-plastic with rigid elastic models in their finite element analysis and found similar results under high speed drilling conditions (Qi, Wang, and Meng 2014). Tuijoft compared the thrust forces required for a constant drill feed rate between cortical and cancellous bone drilling, finding significant differences (10-110 N vs. 3-65 N, respectively) (Tuijthof, Frühwirt, and Kment 2013). This modelling research was less relevant to our objective of measuring the drilled bore depth in bone.

More relevant to our objectives is research done on creating an automatic surgical drill, as this would require detection of layer transition. Many research groups have attempted to automate the drilling process so that the depth of the drilling is not guided purely by the surgeon's intuition of where the drill bit is. This is in contrast to our previous work which used the detecting of drilling tissue level to compute depth of drilled bore, but which was not meant to automate the drilling process (Cavers et al. 2016).

A research group in the UK developed a micro drill for use in middle ear surgery that could detect drill bit breakthrough by analysis of drilling torque and axial load on the drill bit. At that point their device automatically stopped drilling, preventing drill bit plunge (Brett et al. 1995). The anatomy of this region is extremely sensitive and thus precise control of drilling depth is essential. They further refined their concept and developed a robotic surgical drill for use in the OR for preparing cochleostomies (Taylor et al. 2010) and initiated clinical trials

(Coulson et al. 2013). The animal component of their 2013 trial showed 1/20 average velocity of adjacent tissue when compared with conventional methods, demonstrating that their device was able to more accurately detect the breach of the far bone surface and halt the drill than the conventional method.

A separate group in Italy studied the problem of surgical bone drilling in long bones. They first developed and validated a theoretical model for twist drilling of surgical long bones (B. Allotta et al. 1996). In this model they developed an algorithm to detect breakthrough between cortical bone and trabecular tissue or cortical bone and soft tissue based on a threshold axial force. This algorithm was included in a mechatronic drilling tool that stopped automatically at breach of cortical bone, again preventing drill bit plunge (Benedetto Allotta, Giacalone, and Rinaldi 1997). The group then applied wavelet transform analysis to their previous experimental data and were able to detect drill bit breakthrough with a more computationally efficient approach (Colla and Allotta 1998).

Ong et al identified that previous approaches to breakthrough detection relied on relatively homogenous bone density and ignored the influence of system compliance (Ong and Bouazza-Marouf 1998). They showed that system compliance can vary significantly at different anatomic bone locations, and result in different force profiles. To account for these factors they developed a new detection algorithm incorporating a Kalman filter and analysis of force difference between successive samples and drill bit rotation speed that functioned in a more realistic range of settings.

Recognizing that previous automatic drilling systems required replacing the whole drill hand piece at significant expense, Hsu et al developed a modular system that incorporated an

existing drill (Hsu, Lee, and Lin 2001). Their system analyzed the voltage draw of the drill, with high loads associated with drilling cortical bone and low loads with trabecular bone or soft tissue. Similar to previous work this system automatically stopped drilling at breakthrough (Hsu, Lee, and Lin 2001). This work suggests that adding a sensor(s) to an existing surgical drill could detect layer transition without replacing the whole drill handpiece.

Returning to systems requiring a new surgical drill, Lee et al developed a system that allowed for a variable feed rate of the drill assembly – previous systems kept the forward motion of the drill constant. This allowed for a faster drilling process. The feed rate of the drill was controlled by dual force feedback signaling from measurement of drilling force and torque. Their algorithm was based on measurement of drilling torque trend, threshold thrust force, and feed rate (W.-Y. Lee, Shih, and Lee 2004). Subsequently they included a similar control algorithm in a three axis surgical robot for orthopedic drilling (Wen-Yo Lee and Shih 2006).

Louredo et al took a different approach in developing an automatic drilling system. They developed a breakthrough detection algorithm based purely on measurements of the drill bit position that demonstrated superior performance to previous methods involving measurement of force and torque (Louredo, Diaz, and Gil 2012). This algorithm used the difference between an ideal drill position based on a set translational speed and a measured real position, with a control scheme that aimed to minimize the position error. As the drill passed through the cortical bone the position error would increase, and as it neared the end of the cortex there would be less resistance to drilling and the system would accelerate to minimize the error. This acceleration was detected by the algorithm which would stop the drilling process. This algorithm was included in their mechatronic bone drilling system, dubbed

the DRIBON (Louredo, Díaz, and Gil 2012). This work demonstrated that measurement of displacement could be used to detect layer transition in bone drilling.

Bone drilling is a significant part of dentistry in placing oral implants to replace lost teeth. Quest et al developed a system using lasers to ablate the bone, and a laser triangulation sensor to intermittently measure the depth of bore, as part of an automated 'drilling' system (Quest, Gayer, and Hering 2012). This study demonstrated that optical sensing could be done from the surface of bone during a drilling process.

To our knowledge, no previous studies have specifically looked at trying to determine the drilled bore depth in bone automatically.

1.3.4 Porcine Surgical Modelling

Surgery has been simulated in a variety of ways, including using human cadavers, synthetic tissue substitutes, and animal models. Since it is relatively expensive to use human cadaver specimens, we would like to consider using animal models in this study to assess the performance of our laser-based depth gauge.

Pigs have a long history of use in surgical experiments as they are relatively similar to humans in anatomy (Swindle, Smith, and Hepburn 1988). In experimental comparison of bone mineral density and mechanical strength between human bone and various animal models, pig and dog were found to be the most similar to humans (Aerssens et al. 1998). Pigs have been used in a variety of ways for orthopedic surgical education. They have been used in the simulation of osteosynthesis surgery (Leong et al. 2008), arthroscopy (Mattos e Dinato, de Faria Freitas, and Iutaka 2010), and flexor tendon surgery (Smith et al. 2005). We therefore feel that it would be appropriate to use porcine bone models to assess the performance of our system.

1.4 Thesis Overview

In the remaining chapters, we present our device and associated experiments. Chapter 2 presents the Needs Assessment process, which specified the requirements for the device to be built. Chapter 3 overviews the engineering design process that led to our final concept of dual angled sensors measuring from a modified depth gauge. Chapter 4 details the experimental protocol developed to evaluate the repeatability of the design in surgically relevant scenarios. Chapter 5 presents the results obtained from these experiments and Chapter 6 contains the discussion. Chapter 7 offers our conclusions and guidance for future work.

2 Needs Assessment

2.1 Overview

This chapter describes the Needs Assessment for the design of a new laser-based depth gauge for use in surgery on the bony skeleton. The current method for measuring bone bore depth is described, along with its limitations and the clinical context of these measurements. Surgeon interviews and OR observations are reported. I describe the currently used surgical drills and the market share for the major vendors. I also analyze the commonly used surgical incisions and hardware fixation constructs used in osteosynthesis surgery. This information is synthesized to develop a Problem Statement that guided my engineering design.

2.2 Prior Work

A focus group of the UBC Division of Plastic Surgery and the UBC Biomedical Engineering 'Engineers in Scrubs' was held in 2012 to identify problems in current surgical practice that could benefit from the application of engineering design principles. The author co-ordinated this activity from the clinical side, and approximately twenty staff surgeons and ten trainees attended. The current method of measuring drilled bore depth in bone during hand and craniofacial surgery was identified as an area for improvement.

A team of engineering students conducted a preliminary needs assessment and came up with the following problem statement:

"Detecting correct drilled depth is time consuming and incorrect measurement leads to surgical complications".

They then progressed to concept generation, selection, and an initial round of prototyping. In the following section, the Needs Assessment is repeated and expanded to provide a more thorough basis for my design.

2.3 Needs Assessment

2.3.1 Interviews with Practicing Surgeons

I had informal conversations with practicing surgeons who use the conventional depth gauge in their practice. I expanded the scope of the Needs Assessment to include orthopedic surgeons as well as plastic surgeons based on my understanding of surgical practice. The surgeons interviewed were Dr. Pierre Guy in orthopedics, and Dr. Nick Carr, Dr. Alex Seal, Dr. Jim Boyle, and Dr. Erin Brown in plastic surgery. 100% of the surgeons interviewed expressed dissatisfaction with the conventional depth gauge. They said it was difficult to use, time consuming, inaccurate, and at times unusable due to limited surgical exposure (particularly in oral surgery). Notably, specific incidences of wasted screws or inaccurate measurements resulting in need for re-operation, alluded to in the previous needs assessment (and the literature reported in Chapter 1?), were not reported. Surgeons expressed a significant emotional aversion to the current device. All expressed interest in an alternative method of measuring drilled bone bore depth that is more user-friendly.

The plastic surgeons interviewed described using a range of screw sizes from 5-15mm in length. Dr. Guy stated that the longest screw used in orthopedic trauma practice was 85mm.

2.3.2 OR Observations

I went to the OR to observe the depth gauge in use in both orthopedic trauma and plastic surgery contexts. This confirmed the previous understanding of the use of the device.

In practice, the bone is surgically exposed at the site of fracture or osteotomy. An appropriate fixation plate is selected, and the location of the drilled bore for screw placement is selected to match the selected plate. The surgical drill is used to bore through the bone, generally bicortically and nominally perpendicular to the long axis of the bone, though different orientations may be used in selected circumstances. The surgeon notes the feeling of the drill passing through the cortex (slow forward movement of the drill when passing through the cortex, and rapid acceleration at transition to medulla or adjacent soft tissue) and knows the bore is complete when the second cortex has been breached. The drill is removed and the depth gauge is passed through the bore, and then pressed against the side of the bore and pulled back to 'hook' the tip of the gauge on the far cortex. With the tip secure, a measurement can be read from the graduated aspect of the gauge. This measurement is used to select the appropriate screw. Fluoroscopy is used intraoperatively to assess the adequacy of fracture fixation, but not explicitly to confirm the correct screw choice has been made. Occasionally an incorrect screw length is noted intraoperatively with these images and may be corrected with screw replacement, but this is due to chance rather than planning. Routine fluoroscopy has been shown to be inaccurate in detecting wrong-sized screws during routine surgery (Ozer and Toker 2011) and replacing a screw with a new one has been shown to decrease final construct pull-out strength (Matityahu et al. 2013).

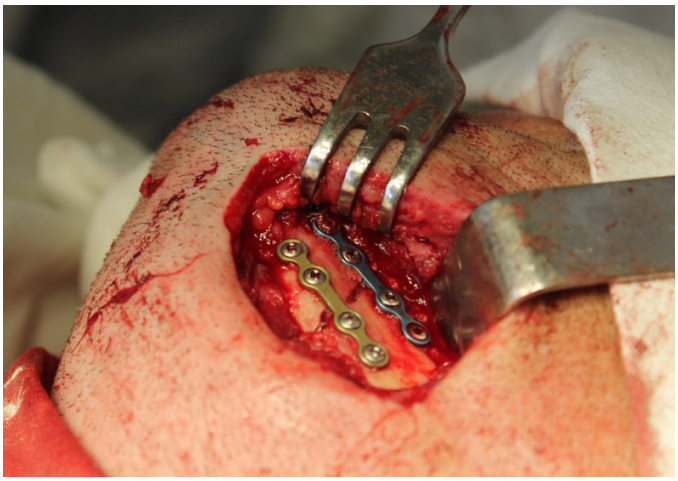

Figure 5– Typical orthopedic surgical exposure with plates and screws in situ

I observed a total of 19 uses of the depth gauge during two surgeries. In three instances the surgeon struggled with the depth gauge. This was due to difficulty in getting the wire component to follow the drilled bore path and hook on the far cortex. This resulted in the process taking more time than usual. No screws were wasted as a result of the device malfunctioning. No screws needed to be removed or replaced during the use of the depth gauge. There was no obvious expense or extra utilization of resources associated with use of the current depth gauge. Theoretically there is a chance that incorrect screw selection based on the measurements of the conventional depth gauge will result in adverse outcomes for patients. There is opinion among surgeons that screws that are too short will result in a suboptimal fracture fixation construct, but there is no evidence this has a clinical effect.

2.3.4 Updated Needs Statement

I synthesized the information from the previous work, and the confirmatory conversations with surgeons and observations made in the OR to draft a new 'Needs Statement.'

"There is a need for a device to measure drilled bore depth in bone during surgery that is more accurate, less time consuming, and less frustrating for the surgeon than the current depth gauge approach."

2.4 Context Identification

2.4.1 Clinical Uses of the Depth Gauge

I assessed the use cases of the conventional surgical depth gauge based on my knowledge of surgical technique from previous training and review of appropriate surgical textbooks. This assessment was corroborated in conversation with senior orthopedic (Dr. Pierre Guy) and plastic surgeons (Dr. Nick Carr and Dr Kevin Bush). The depth gauge is needed in any surgical case where components of bone are to be attached using plates and screws, and when the length of screw is to match the length of available bone. Use cases of the depth gauge are summarized below. Areas of orthopedic surgery not included, because the depth gauge is not used, are arthroplasty, spine surgery, and pelvis surgery.

Orthopedic Surgery: upper and lower extremity trauma

Plastic Surgery: hand trauma, craniofacial trauma, osseous reconstruction

Oral and Maxillofacial Surgery: orthognathic surgery

Other: Veterinary surgery, rib and sternal fixation

I obtained information from the Vancouver General Hospital (VGH) Business Manager, Meilan Robson, about the total number of these cases performed at VGH per year to estimate the size of the market for depth gauges. VGH is a quaternary care acute hospital with approximately 700 beds and 23 000 inpatient and outpatient surgical cases per year. In the

2015/2016 fiscal year 1087 surgical cases would likely have used the depth gauge. The distribution among different surgical services is shown in the figure below, with orthopedic trauma being the largest user of the depth gauge.

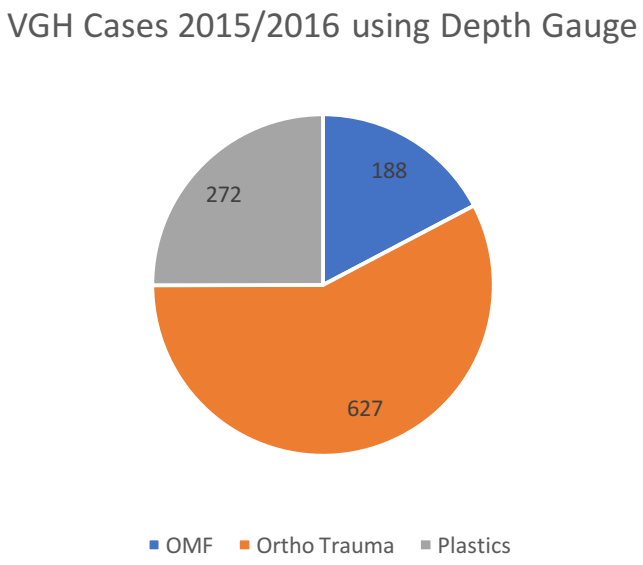

Figure 6 – Distribution of surgical cases using the depth gauge between different services at VGH

2.4.2 Surgical Drills

Surgical drills come in two main types: pistol type and pencil type. Orthopedic surgeons exclusively use pistol type drills, while oralmaxillofacial (OMF) surgeons tend to use pencil type. Plastic surgeons generally use pistol type drills, though some will use pencil type for operations on the facial skeleton as a matter of preference. There is no clear superiority of one type over another, and different use patterns tend to reflect the predominantly used device where the surgeon trained. Orthopedic trauma surgeons, which as shown in the above section perform most of the operations involving the depth gauge, use exclusively pistol type surgical drills.

Figure 7 – Pistol type drill

Figure 8 – Pencil type drill

Drills are classified by size and power as small bone, medium bone, and large bone. Large bone drills are used for orthopedic reconstructive procedures that do not require use of the depth gauge, so they will be omitted from further analysis. In North America the majority of surgical drills are sold by Stryker and Linvatec (personal communication with Stryker Sales Representative Darren Harris). Market size and share for small and medium bone surgical drills are shown in the figures below.

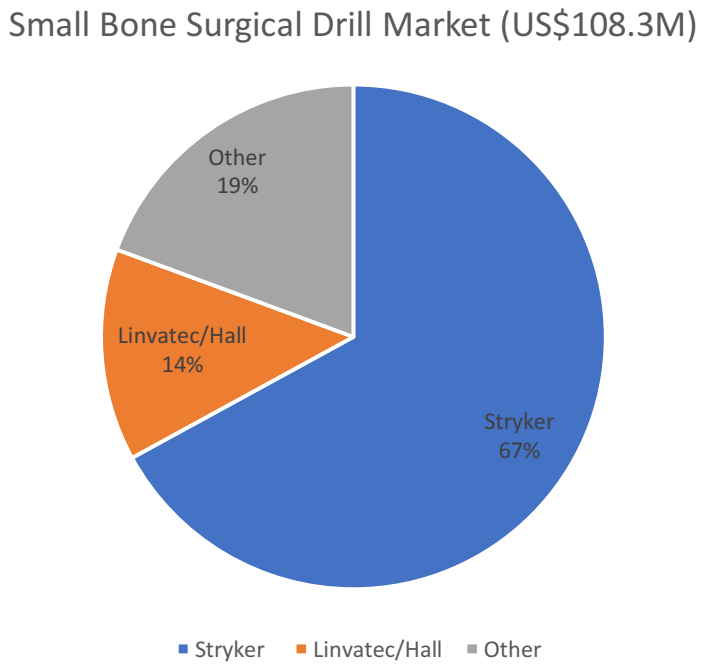

Figure 9 – Small Bone Drill Market USA 2015

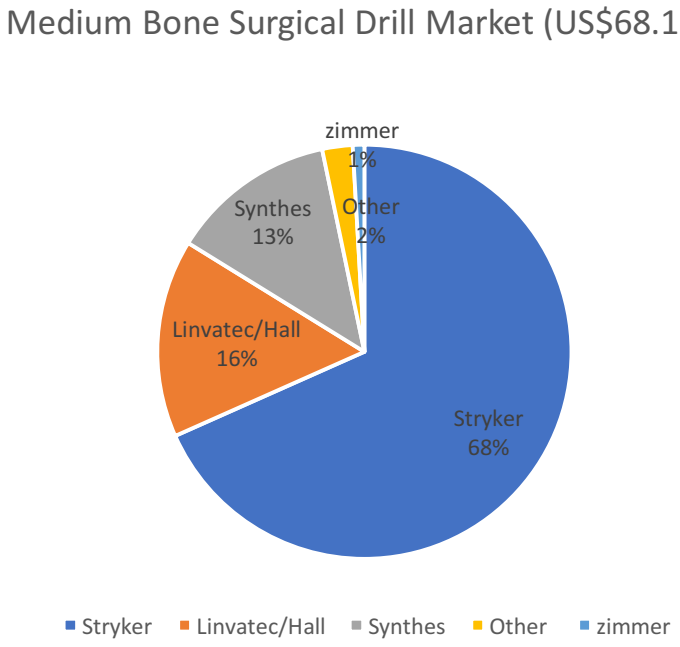

Figure 10 – Medium Bone Drill Market USA 2015

Stryker and Linvatec combined account for more than 80% of both the small and medium bone market.

2.4.3 Surgical Screws

Surgical screws come in standard lengths with the instrument sets for the various indications (oral maxillofacial, orthopedic trauma). Shorter screws increase in increments of 1 mm, and the increments get larger as the screws get longer. A selection of different screw lengths available for different indications are shown in the tables below (Stryker product catalogues).

2.0mm Self-Tapping

2.0 x 6mm screw/illustrated scale 2:1

Non-Sterile 5/ea. Pack	Length
50-20404	2.0 x 4mm
50-20405	2.0 x 5mm
50-20406	2.0 x 6mm
50-20407	2.0 x 7mm
50-20408	2.0 x 8mm
50-20410	2.0 x 10mm
50-20412	2.0 x 12mm
50-20414	2.0 x 14mm
50-20416	2.0 x 16mm
50-20418	2.0 x 18mm
50-20420	2.0 x 20mm

Figure 11 – Mandible Screws from Stryker

1.2mm Self-Tapping

1.2 x 6mm screw/illustrated scale 2:1

Non-Sterile 5/ea. Pack	Length
50-12003	1.2 x 3mm
50-12004	1.2 x 4mm
50-12005	1.2 x 5mm
50-12006	1.2 x 6mm
50-12007	1.2 x 7mm
50-12008	1.2 x 8mm
50-12010	1.2 x 10mm
50-12012	1.2 x 12mm

Figure 12 – Upper Face Screws from Stryker

5.0MM LOCKING SCREWS, SELF TAPPING T20 DRIVE

Stainless Steel REF	Length mm
371314	14
371316	16
371318	18
371320	20
371322	22
371324	24
371326	26
371328	28
371330	30
371332	32
371334	34
371336	36
371338	38
371340	40
371342	42
371344	44
371346	46
371348	48
371350	50
371355	55
371360	60
371365	65
371370	70
371375	75
371380	80
371385	85
371390	90
371395	95

Figure 13 - Orthopedic trauma screws from Stryker

2.4.4 Surgical Exposure Dimensional Analysis

Because Orthopedic trauma surgery of the appendicular skeleton represents the largest usage for depth measurement, I concentrated on assessing these applications. To characterize the geometry of these use case scenarios, I conducted a dimensional analysis of surgical approaches to the appendicular skeleton commonly performed in orthopedic surgery. My goal is to use this knowledge of the surgical exposure geometry in evaluating potential configurations of the laser-sensing device on the surgical drill (eg, establishing the optimal position and orientation of the sensor).

Accurate dimensions of the incisions used in orthopedic surgery have not, to my knowledge, been analyzed or reported in the orthopedic literature. Surgery may be described with reference measurements to anatomic landmarks, but the dimensions of the final incisions or the area of bone exposed have not been described. However accurate images of the surgical exposures are available in surgical textbooks, and I used these as the basis for this investigation.

I used the '*Atlas of Surgical Exposures of the Upper and Lower Extremity*' by Tubiana et call (Martin Dunitz Ltd. 2000). This textbook provides detailed illustrations of the incisions and exposures used in orthopedic surgery, as well as visual references to the size of the incisions on the human body. I reviewed all images in the text, and selected those used in orthopedic trauma surgery and likely to require use of the depth gauge (n = 28). This knowledge comes from my training in surgery, as well as conversation with staff orthopedic surgeon Dr. Pierre Guy.

I analyzed the selected images for dimensionless proportions using Adobe Photoshop (Adobe, USA). I took measurements of the length and width of the incision, as well as the length and width of the exposed bone (see Figure 14). An estimated 'true' length of incision was obtained by reviewing the indicated incision marking in the text and then measuring the corresponding length on a human volunteer. The proportion between this value and the dimensionless incision length from the Photoshop analysis was used to compute a correction factor, which could then be used to calculate the predicted values for the other exposure dimensions.

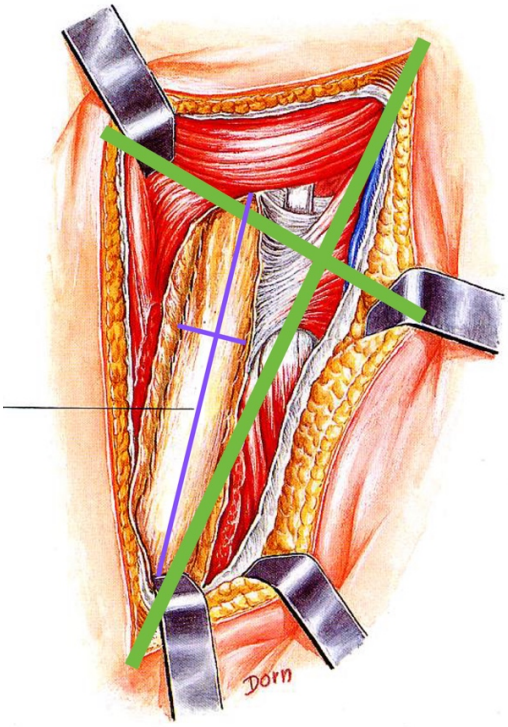

Figure 14 – Surgical exposure dimensional analysis. Incision dimensions are indicated in green, and bone exposure dimensions are indicated in purple.

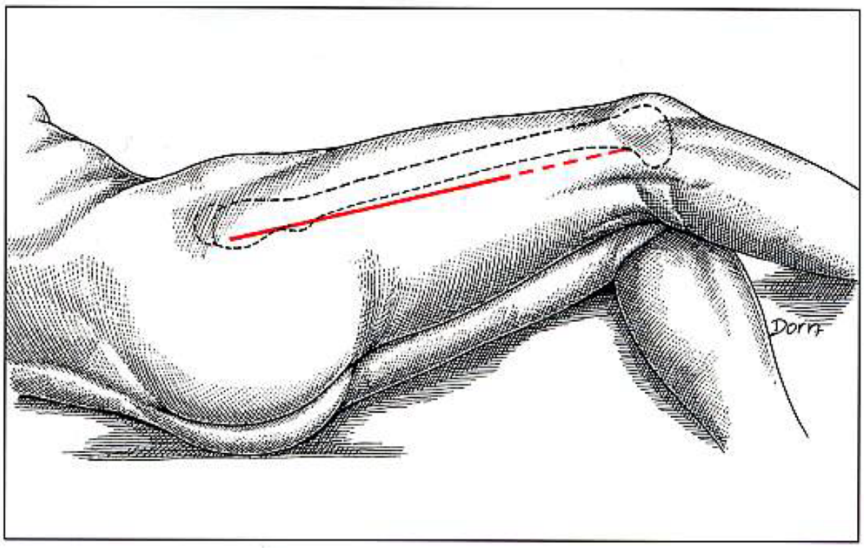

Figure 15 - Example of incision marking image

A summary of the data is presented in Table 1. Data is presented in Appendix A.

	Length (cm)	Std. Dev.	Width (cm)	Std. Dev.
Incision	18.5	5.3	8.8	3.3
Bone	11.4	4.1	1.9	0.8

Table 1 – Dimensional Analysis Summary

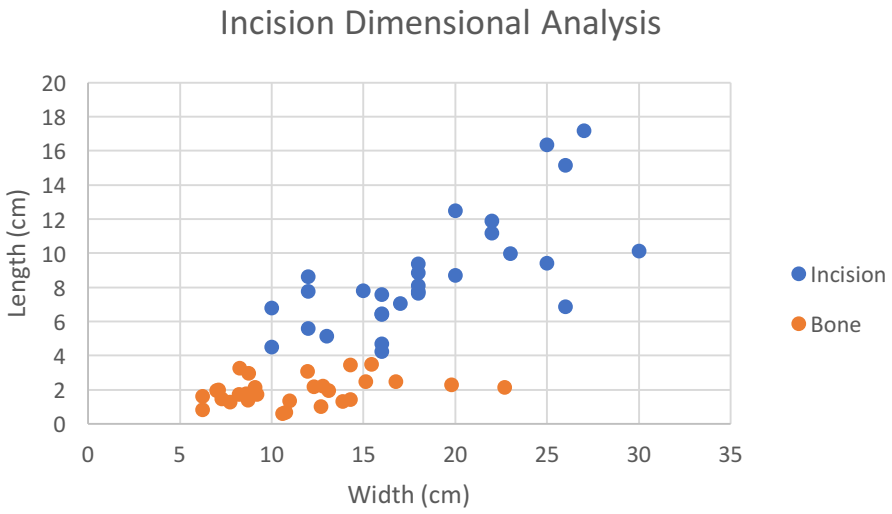

Figure 16 – Plot of the Incision Dimensional Analysis

2.4.5 Fixation Construct Analysis

I also performed a detailed descriptive analysis of the physical arrangement of the bone, plates, and screws in fracture fixation constructs to clarify the use case environment for bore depth drilling. The AO Surgical Reference(Colton et al. 2017) is an online resource that includes instructions and schematics for performing orthopedic trauma surgery. I reviewed all the described procedures, and identified those that involve use of the depth gauge. A total of 63 different fixation constructs with 520 screws were relevant based on my prior review of the use case, discussions with practicing surgeons, and my surgery training.

The conditions of each screw were classified based on section of bone (diaphyseal or metaphyseal) and orientation of the screw relative to the bone surface (perpendicular or angled) at entry and exit from the bone. Unicortical screws were noted in the construct analysis but only bicortical screws were included in determining construct types, as depth measurement is principally relevant when using bicortical screws. I used this information to

classify the screw-bone relationship into four types, depicted in the figures below. Data tables are available in the Appendix B.

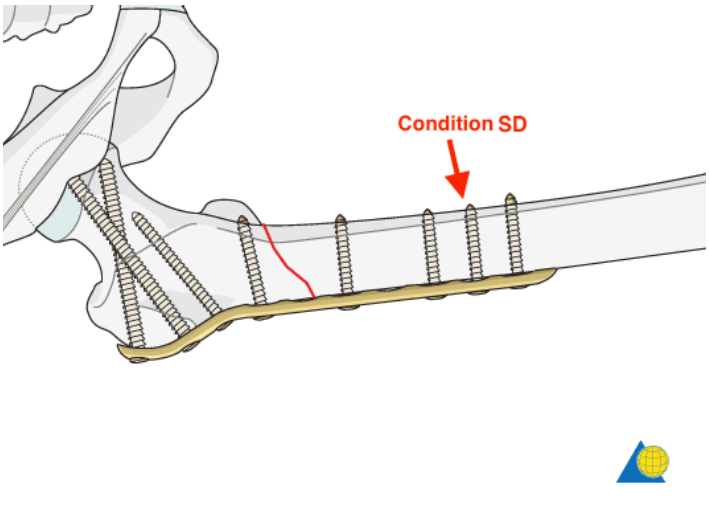

Figure 17 - Condition SD (straight diaphysis), perpendicular drilling to long axis in diaphyseal bone. Perpendicular entry and exit of screw relative to bone surface.

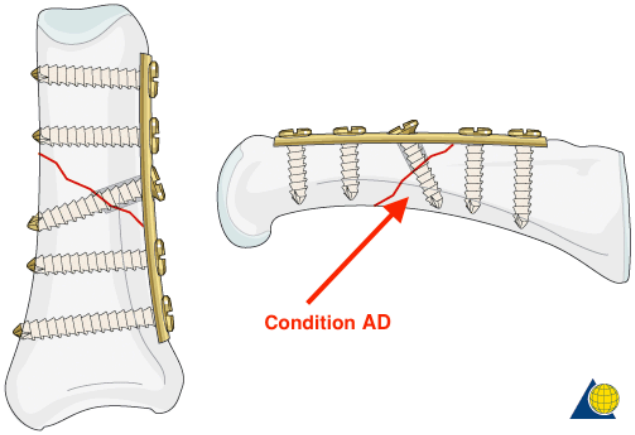

Figure 18 - Condition AD (angled diaphysis), angled drilling to long axis in diaphyseal bone. Angled entry and exit of screw relative to bone surface

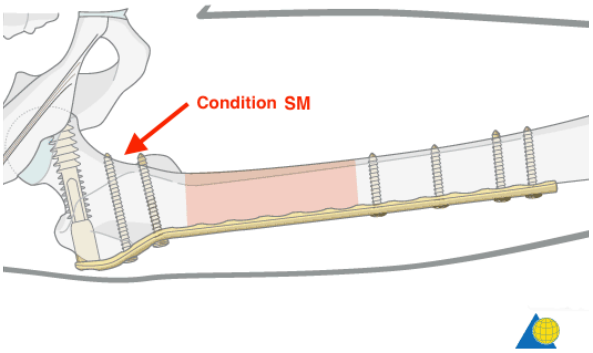

Figure 19 - Condition SM (straight metaphysis), perpendicular drilling to long axis in metaphyseal bone, angled entry and exit relative to bone surface

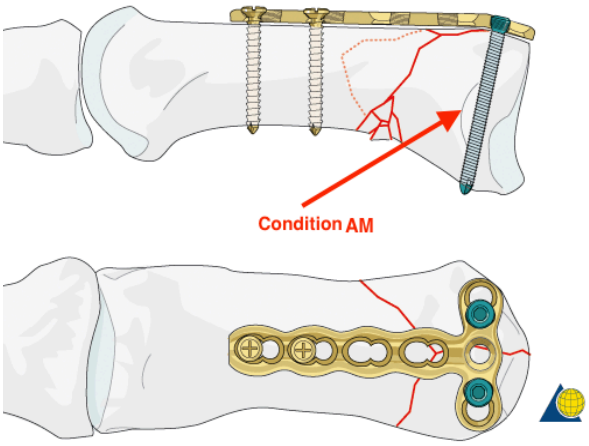

Figure 20 - Condition AM (angled metaphysis), angled drilling to long axis in metaphyseal bone, perpendicular entry and angled exit relative to bone surface

The relative number of screws classified into each conditions is shown in Figure 21.

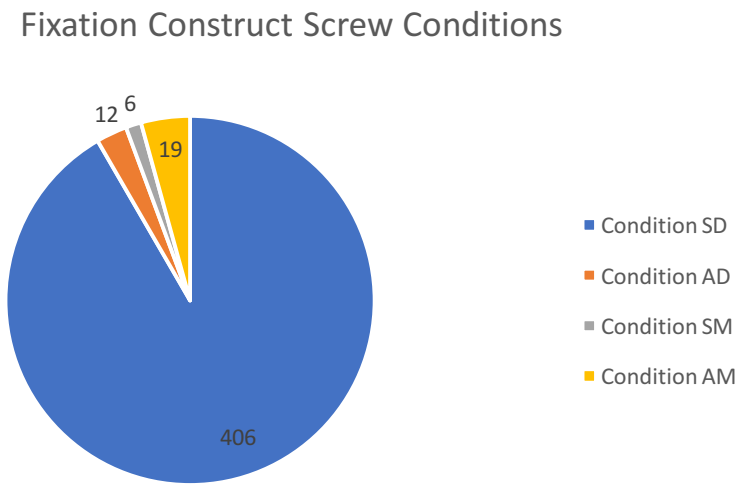

Figure 21 - Screw conditions in Construct Analysis

2.4.6 Current Surgical Depth Gauge

The standard form of the surgical depth gauge has not changed significantly since that described by Gunther in 1948 (Gunther and Keyes 1948). The basic design is a thin wire shaft of known length with a hooked end that is passed through the drilled bore. The hooked end engages with the far cortex as the gauge is retracted, and gradations on the length of the gauge shaft are used to measure the depth of the instrument and the bore.

It can be difficult to engage the hooked end of the gauge with the far cortex, resulting in delays in obtaining a measurement. The passage of the instrument is not visualized (a 'blind' procedure) so it can be challenging to orient the instrument.

2.5 Problem Statement

Information from the past work, the new Needs Assessment process, and the Context Identification results were synthesized to develop a problem statement to guide our design:

The objective is to develop a device that will measure the depth of drilled bore in bone during surgery reliably to an accuracy of 1mm, is compatible with the most commonly used pistol type surgical drills, does not require a separate measurement step, and does not add significantly to the cost per surgical case.

3 Design

3.1 Overview

In this section I outline the design process taken in developing a replacement for the conventional depth gauge in bone surgery. I decided to use the same measurement concept as the prior work, with continuous displacement measurement of the drill relative to the bone as the analyzed signal. I did a Functional Structural Decomposition to identify the necessary components for the final device. All the necessary components for a final device are discussed in the initial design phases, and then a more limited number are taken forward to feasibility and reliability testing. The Prototyping section describes the prototypes developed to test the different arrangements of laser sensors for displacement measurement that are tested in the Experimental section.

3.2 Problem Statement

The objective is to develop a device that will measure the depth of drilled bore in bone during surgery reliably to an accuracy of 1mm, is compatible with the most commonly used pistol type surgical drills, does not require a separate measurement step, and does not add significantly to the cost per surgical case.

3.3 Concept

The forward movement of the drill along its drilling axis, relative to a fixed surface, is the same as the forward movement of the drill bit as it bores through the bone. Therefore, the change in displacement of the drill relative to a fixed surface in front of it between the point of

drilling initiation and that of breach of the far cortex is the same as the depth of the drilled bore. This is shown in Figure 22.

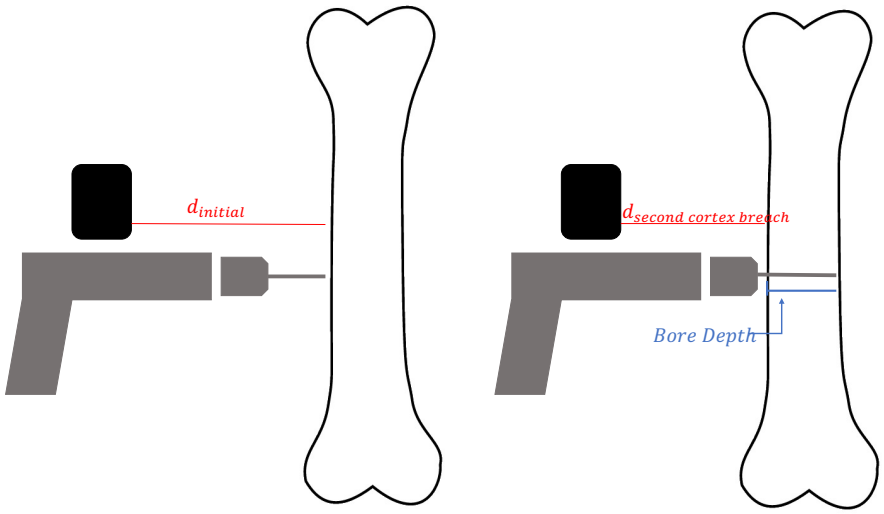

Figure 22 - Relationship between displacement measured and bore depth

$$Bore\ Depth\ = d_{second\ cortex\ breach} - d_{initial}$$

Differentiation and double differentiation of the displacement signal gives the velocity and acceleration, respectively. Drilling through the cortical bone is essentially uniform at low velocity, followed by a rapid acceleration when the cortex is breached. This acceleration happens twice in bicortical drilling, first in the transition between the cortex and the medullary canal and again when breaching the second cortex into the adjacent soft tissue. The time point of rapid increase in velocity and acceleration therefore corresponds to the cortex breach, and can be used to identify the displacement at that point. This allows computation of the drilled bore depth.

A typical displacement, velocity, and acceleration tracing is shown in Figure 23.

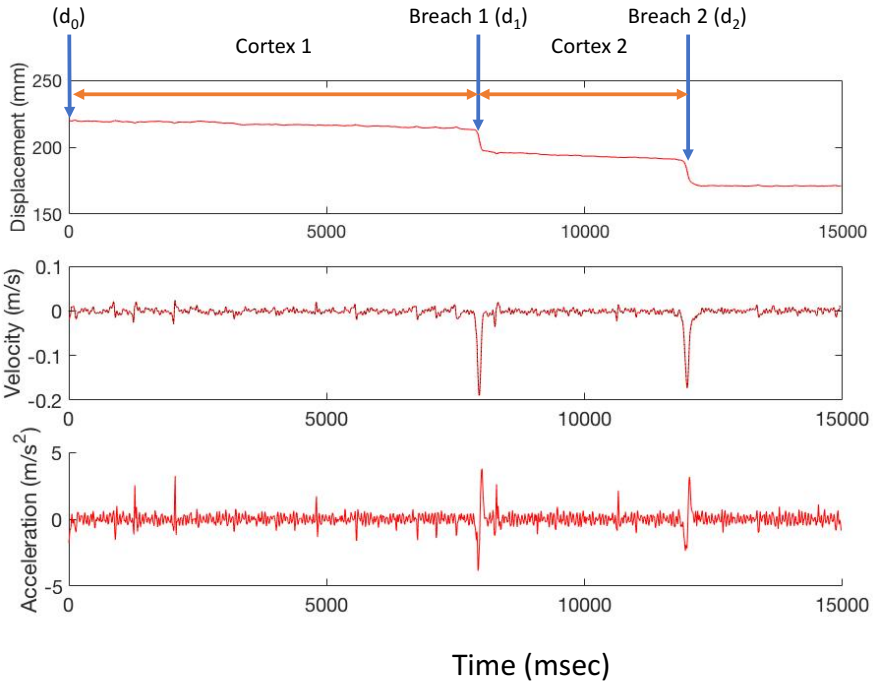

Figure 23 - Graph of measured displacement and computed velocity, acceleration during bore drilling

This concept was shown to be effective (Cavers et al. 2016) and has advantages related to the design objectives outlined below – specifically that it supports compatibility with existing surgical drills.

3.4 Design Specifications

The following key specifications arising from the need identification process are labeled with an (R) if it represents a requirement, and with (EC) if it represents an evaluation criterion.

Functional

- Device provides measurement of drilled bore in bone to an accuracy of +/- 1mm (R)
- Device will measure holes up to 10cm depth (R)

Economic

- Device is inexpensive (<$300 /case used) (EC)

Durability

- Device is compatible with sterile operating conditions (R)

Ergonomic

- Device is compatible with right or left handed use (R)
- Use of device is appealing to surgeons, as defined by user experience study (EC)

Input/Output Constraints

- Device is compatible with currently used surgical drills in North America (EC)

Regulatory

- Device can be approved through FDA 510k regulatory process (R)

3.5 Functional Structural Decomposition

A block diagram of the device architecture is shown in Figure 24. The sensor, drill mount assembly, and computer system were present in basic form in the previously developed design. These components require further development to produce a final device. Additionally, a user interface, battery power supply, and a housing compatible with the sterile operating room environment are required for the final form of the device.

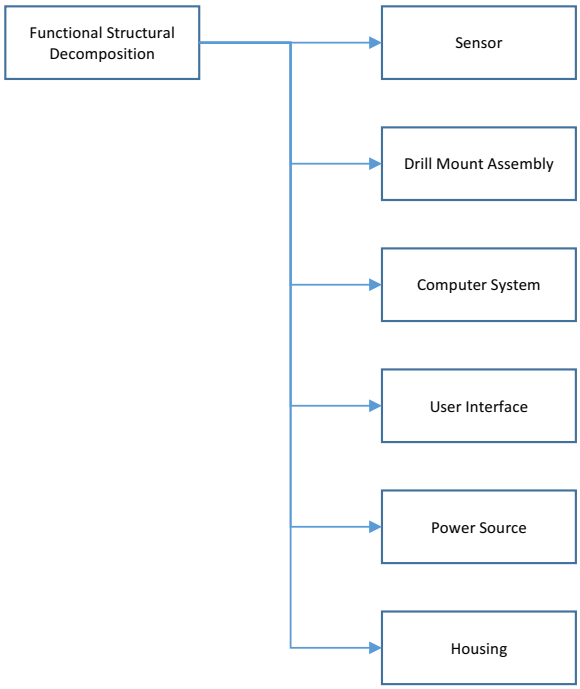

Figure 24 – Device architecture diagram

3.6 Sensor

3.6.1 Concept Selection

Prior work used a mechanical approach to measure displacement of the drill relative to the bone, with a sliding measurement arm and a linear potentiometer. To improve this design, I decided to explore optical distance sensing for measurement of the displacement. Removing the need for a mechanical arm reduces the intrusion of the device into the operative field, improving the user experience. It is also less dependent on the geometry of the surgical drill, which could be helpful in achieving compatibility with multiple drill models.

3.6.2 Optical Sensing

Multiple methods of optical sensing are described in the literature and used in engineering practice. These include intensity-based sensors, triangulation sensors, time of

flight sensors, confocal sensors, and interferometric sensors (Berkovic and Shafir 2012). A summary of the range and resolutions of the commonly used techniques in commercial use is shown in Table 2. Based on the target measurement range (up to 10cm of drilling depth) and desired resolution (precision to within 1mm) laser triangulation is most appropriate for the device.

Method	**Range**	**Resolution**	**Notes**
Intensity-based	5-50 mm	1 µm	Sensitive to change in surface conditions
Triangulation	10 mm – 1 m	Several µm	Resolution can change across working range
Time of Flight	Long (km +)	1 cm	RADAR
Confocal	Several mm	Sub µm	Used to build confocal microscopes

Table 2 – Summary of common optical distance sensing method properties

3.6.3 Laser Triangulation

Laser triangulation sensors are used frequently in industry as part of manufacturing systems. They can provide continuous, high resolution measurements of the displacement of manufactured parts from machine tools and robots. Off the shelf devices exist for different measurement ranges and resolutions.

SPECIFICATIONS

Sensor heads

Model		IL-030	IL-065	IL-100	IL-300	IL-600	IL-2000
Appearance							
Reference distance		30 mm 1.18"	65 mm 2.56"	100 mm 3.94"	300 mm 11.81"	600 mm 23.62"	2000 mm 78.74"
Measurement range		20 to 45 mm 0.79" to 1.77"	55 to 105 mm 2.17" to 4.13"	75 to 130 mm 2.95" to 5.12"	160 to 450 mm 6.30" to 17.72"	200 to 1000 mm 7.84" to 39.37"	1000 to 3500 mm 39.37" to 137.80"
Light source		Red semiconductor laser, wavelength: 655 nm (visible light)					
	Laser class	Class 1 (FDA (CDRH) Part1040.10) [1.] Class 1 (IEC 60825-1)	Class 2 (FDA (CDRH) Part1040.10) [1.] Class 2 (IEC 60825-1)				
	Output	220 µW	560 µW				
Spot diameter (at standard distance)		Approx. 200 × 750 µm	Approx. 550 × 1750 µm	Approx. 400 × 1350 µm	Approx. ø0.5 mm ø0.02"	Approx. ø1.6 mm ø0.06"	Approx. 1400 x 7000 µm
Linearity [2. 3.]		±0.1% of F.S. (25 to 35 mm 0.98" to 1.38")	±0.1% of F.S. (55 to 75 mm 2.17" to 2.95")	±0.15% of F.S. (80 to 120 mm 3.15" to 4.72")	±0.25% of F.S. (160 to 440 mm 6.30" to 17.32")	±0.25% of F.S. (200 to 600 mm 7.84" to 23.62") ±0.5% of F.S. (200 to 1000 mm 7.84" to 39.37")	±0.16% of F.S. (1000 to 3500 mm 39.37" to 137.80")
Repeatability [4.]		1 µm	2 µm	4 µm	30 µm	50 µm	100 µm
Sampling rate		0.33/1/2/5 ms (4 levels available)					
Operation status indicators		Laser emission warning indicator: Green LED, Analog range indicator: Orange LED, Reference distance indicator: Red/Green LED					
Temperature characteristics [3.]		0.05% of F.S./°C	0.06% of F.S./°C	0.06% of F.S./°C	0.08% of F.S./°C		0.016% of F.S./°C
Environmental resistance	Enclosure rating	IP67					
	Ambient light [5.]	Incandescent lamp: 5000 lux	Incandescent lamp: 7500 lux		Incandescent lamp: 5000 lux		Incandescent lamp: 10000 lux
	Ambient temperature	-10 to +50°C 14 to 122°F (No condensation or freezing)					
	Relative humidity	35 to 85% RH (No condensation)					
	Vibration	10 to 55 Hz Double amplitude 1.5 mm 0.06" XYZ each axis: 2 hours					
	Pollution degree	3					
Material		Housing material: PBT, Metal parts: SUS304, Packing: NBR, Lens cover: Glass, Cable: PVC					
Weight		Approx. 60g	Approx. 75g		Approx. 135g		Approx. 350g

1. The laser classification for FDA (CDRH) is implemented based on IEC 60825-1 in accordance with the requirements of Laser Notice No.50.
2. Value when measuring the KEYENCE standard target (white diffuse object).
3. F.S. of each model is as follows. IL-030: ±5 mm ±0.20" IL-065: ±10 mm ±0.39" IL-100: ±20 mm ±0.79" IL-300: ±140 mm ±5.51" IL-600: ±400 mm ±15.75"
4. Value when measuring the KEYENCE standard target (white diffuse object) at the reference distance, sampling rate: 1 ms, and average number of times: 128. For the IL-300/IL-600, the sampling rate is 2 ms.
5. Value when the sampling rate is set to 2 ms or 5 ms.

Table 3 – Laser displacement sensors available from KEYENCE

3.6.4 Sensor Orientation

Multiple orientations of the displacement sensor relative to the drilling axis are theoretically compatible with the measurement of drilled bore based on the displacement signal. The core idea is illustrated in Figure 25 – here, the laser beam is directed parallel to the drilling axis. As long as the drill remains in the same orientation throughout the drilling cycle, the laser spot on the anatomy will remain in the same place, and the resulting depth estimate will be accurate. However, if the drill tilts or the point where the laser hits moves relative to the bone during drilling, an error can be introduced.

To compensate for the tilting effects, we could mount displacement sensors on opposite sides of the drill (see Figure 25) and average the resulting measurements from the different sensors, which would significantly reduce the sensitivity of the measurement to tilt, though the system's

depth measurement would remain vulnerable to relative movement between the laser spots and the bone.

The laser beam could also be angled, as shown in Figure 26, to reduce the distance between the drill axis and the laser spot, though this would mean that the laser spot would translate laterally during drilling; if the surface were not perpendicular to the drill axis, this would produce a depth measurement error.

In practice, the majority of drilling is done using a drill guide, as shown in Figure 27. By adding a protrusion to the guide that the laser spot could land on, we could ensure that the spot always remains in the same position, which would significantly reduce sensitivity to drill tilt.

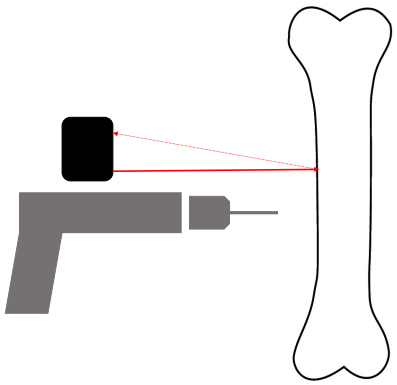

Figure 25 - Displacement sensor collinear with drilling axis, measuring from tissue surface

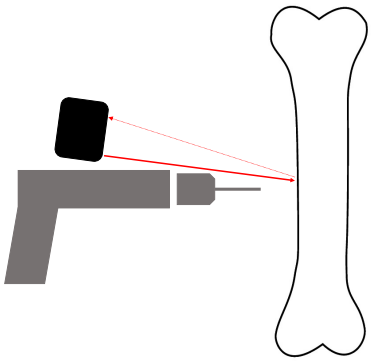

Figure 26 - Displacement sensor angled relative to drilling axis, measuring from tissue surface

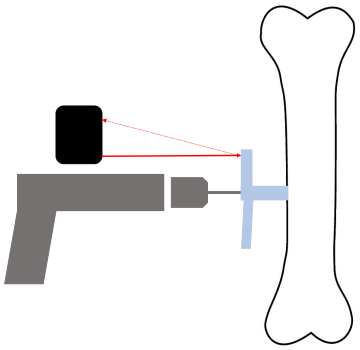

Figure 27 - Displacement sensor, collinear or angled, measuring from fixed surface such as drill guide

3.7 Microprocessor

The analogue output signal of the displacement sensor is sent to a microprocessor unit (see Prototyping, below). In the final design the microprocessor will compute the bore depth based on an algorithm and output the value to the display component of the user interface – a 'standalone' device. The microprocessor must communicate with the user interface. This must allow for both display of computed bore depth and for device control. For testing purposes, we do not need the information to be processed in real time, so we are currently storing the data on a data card and processing it post facto.

3.8 Algorithm

In the final form the algorithm would run on the device microprocessor and compute the drilled bore depth by detecting cortical breach based on the spike in velocity and/or acceleration. The algorithm must be able to account for noise in the signal and the measured values associated with routine surgical use. Most likely the algorithm would detect when the drill exceeded a threshold for velocity and/or acceleration and identify that point as the cortical breach.

3.9 User Interface

A device that functions in real-time would need a display that shows the computed bore depth to the surgeon after drilling the bore in the bone. The system would have to be activated in some way to begin measuring displacement, either through a controller or by some passive detection system.

In my experiments I developed prototypes that required post processing, and did not go through the detailed steps to determining what components would be necessary for a real-time design.

3.10 Mounting Assembly

The device is to be compatible with existing surgical drill stock. Therefore, the mounting assembly must allow secure attachment of the device to existing drills with variable geometry. It must be secure enough that the alignment of the sensor is not disrupted during surgical use, and the mounting step must be simple and quick. Based on the analysis of existing drills performed in the 'Needs Assessment' the preliminary concept for this function is a 'clamp' method that affixes the device to the superior aspect of the drill body.

3.11 Power Supply

The device must be battery powered, as a cord would not be compatible with operating room sterile technique. There must be sufficient energy storage for use for an entire surgical case, which typically lasts 90 minutes but in more complicated circumstances could last in the range of 240-300 minutes. A typical case will involve measuring 5-10 bore depths, but 20 bore depths is possible.

3.12 Housing

The internal electrical components of the device must be encased in a housing that can be sterilized for use in the operating room. The housing thus must be water and vapor-proof, both for the sterilization process and for the surgical environment, where the device will be exposed to blood and aqueous fluids. The housing must either protect the electrical components from the sterilization process, or create a barrier between the operating environment and non-sterile electrical components inserted into the housing at the time of surgery. A reusable or disposable housing design are both possible.

3.13 Prototyping

The objective of the prototyping phase of the project was to demonstrate the feasibility and reliability of laser triangulation in the displacement sensing concept for automatic measurement of drilled bore in bone. I tested multiple concepts of sensor number and orientation. These early prototypes required data post-processing and analysis on a computer, and did not address user interface or sterilization issues. Four sensor arrangements were developed and tested.

Pilot testing was done on each of the prototypes to assess performance and drive further design efforts. The results of these experiments are summarized in Chapter 4. A discussion on the performance of each sensor arrangement is presented in Chapter 5.

3.13.1 Single sensor, parallel to drilling axis, measuring from tissue

The initial sensor used in the design was a KEYENCE IL-300 laser displacement sensor. It has a reference distance of 300mm and a range of 160 – 450 mm. Measurement repeatability is 30 μm and the sampling rate is controllable between 0.33 and 5 ms. There are multiple

outputs for electronic integration of the sensor, and we used the 0-5 V analogue output. This sensor was chosen because it had an appropriate measurement range, but its resolution was better than we required and was quite costly (~$2500), so we would not likely use this specific device in a future commercial system. Nonetheless, we deemed it suitable for evaluating the fundamental concept.

The sensor was mounted on an aluminum frame, which included an adjustable C-clamp for drill attachment. The assembly was mounted on a ConMed MPower2 medium size pistol type surgical drill, with the device positioned superior to the drill body (see Figure 28).

Figure 28 – Single parallel sensor prototype

In our early stage prototype the microprocessor output time and displacement values via USB to a personal computer running MATLAB (Mathworks, USA). Initially the device used an Arduino UNO microprocessor (10 bit ADC), and later I switched to an Arduino DUE (12 bit ADC) for better resolution(Arduino, Italy). The flow diagram for data and the accompanying software is shown in Figure 29. A basic circuit diagram of the prototype is shown in Figure 30.

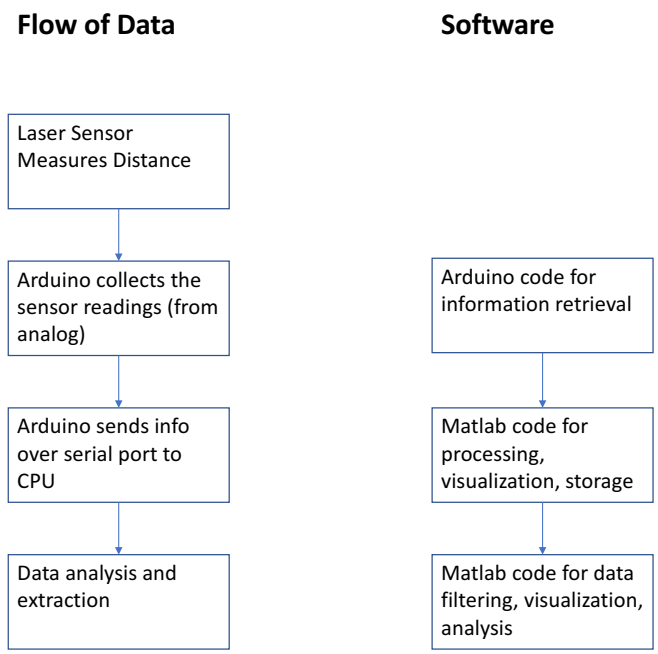

Figure 29 – Data and software flow chart

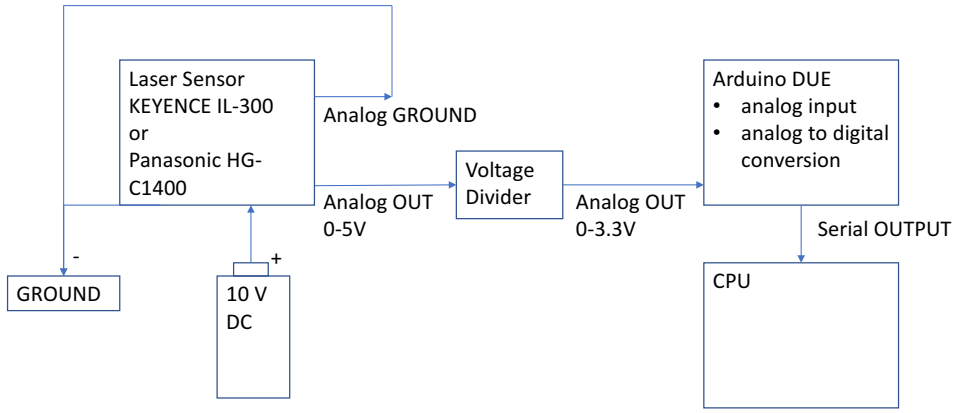

Figure 30 – Prototype circuit diagram

In the early stage prototype, we used MATLAB code for data filtering and visualization, with manual interpretation. The code was the time limiting step in the process, and allowed for a sampling frequency of 100 Hz. Initial data was quite noisy, so a signal processing step was added using MATLAB's Signal Processing Toolbox.

Butterworth filters are effective in filtering noise from human kinematic movements(Winter, Sidwall, and Hobson 1974). We chose a second order Butterworth filter with a cutoff frequency of 10 Hz. Cutoff frequency was selected based on Fast Fourier Transform Analysis and review of the resulting periodogram. A sample periodogram is shown in Figure 31.

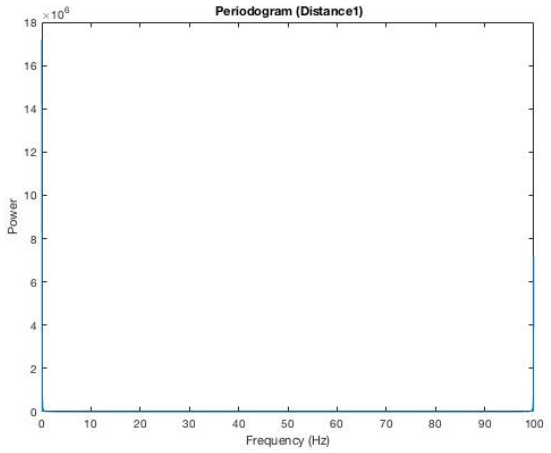

Figure 31 - Periodogram for displacement

Bore depth was determined by graphical interpretation of the filtered displacement data. Figures showed a typical initial period of minimal change in displacement associated with drilling of the first cortex, followed by a rapid change associated with breaching the cortex and passing through the medulla. There was then another period of minimal change associated with drilling the second cortex, and another rapid change associated with breaching the second cortex. This is shown in Figure 23.

3.13.2 Dual sensor, parallel to drilling axis, measuring from tissue

To address the sensitivities to tilt found in the single collinear design presented above, I added a second laser displacement sensor on the opposite side of the drilling axis to the first.

Rather than simply replicating the expensive Keyence sensor, I chose instead to use a Panasonic HG-C1400 sensor ($600). It has a reference distance of 400 mm, a measurement range of 200 – 600 mm, a repeatability of 300 – 800 μm (range dependent; better at the low end of the range where we expect to be making our measurements), and a controllable sampling rate between 1.5 – 10 ms. These performance parameters are expected to be acceptable for our application. Computing and software was the same as the previous prototype. The measured bore depth was taken as the average of the values determined by the two sensors. The prototype is shown in Figure 33.

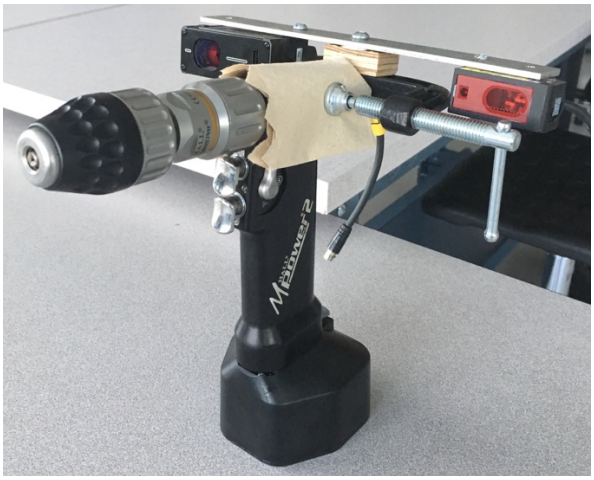

Figure 32 – Dual parallel sensor prototype

3.13.3 Dual sensor, angled towards drill bit, measuring from tissue

Reliability issues were still present in the dual sensor parallel design, so I made the further modification of angling the beams towards the drilling axis. This would limit the effect of rotation or tilt of the drill on the displacement measures of the sensors (see Discussion), as well as make it more feasible to measure from the surface of the bone rather than adjacent soft tissue. Computation and software were the same as in the previous prototype, though a correction factor had to be applied to the displacement measurement due to beam angle.

Determination of the correction factor is shown in Figure 34. The prototype is shown in Figure 35.

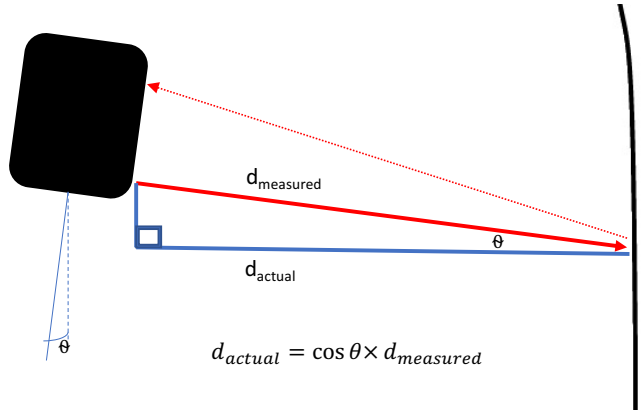

Figure 33 – Correction for beam angle

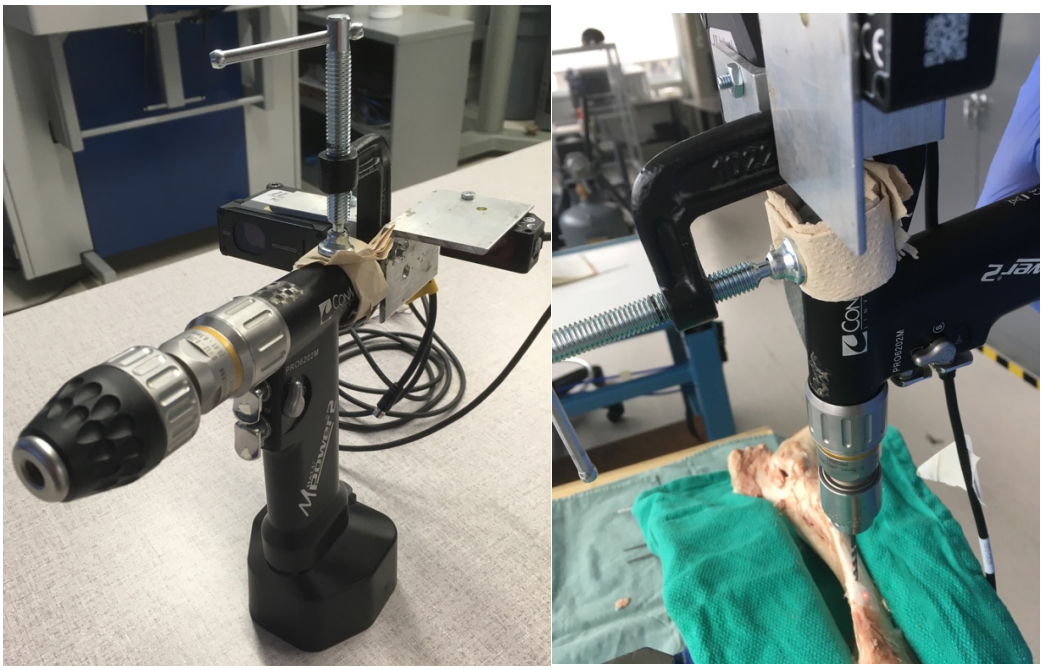

Figure 34 – Dual sensor, angled towards drill bit

3.13.4 Dual sensor, angled towards drill bit, measuring from drill guide

Previous prototypes took displacement measurements from the tissue, either bone or muscle. This is an irregular surface, and vibration or rotation of the drill hand piece could result in fluctuations in measured displacement not associated with forward motion of the drill.

Fluctuations would be due to the beam moving over curved bone or tissue surfaces, or encountering tissue debris. To minimize this source of error I tested the previous dual angled sensor prototype with a simulated drill guide. A drill guide is used in many situations in orthopedic surgery to give more control of drill trajectory, and a feature could easily be added to provide a smooth, constant surface for displacement measurement. In our pilot studies, the drill guide was kept 'flush' and fixed relative to the bone during use (see Discussion). I simulated this by using a 4 cm x 10 cm x 1.5 cm piece of aluminum, with a drilled hole the same size as the orthopedic drill bit. The bit was passed through this hole prior to drilling, and then the drill guide was seated snuggly against the bone surface. The drill guide remained fixed relative to the bone, and the sensors were oriented to read displacement from its surface. In this way the displacement was measured from a regular surface and was less sensitive to vibratory or rotational movements of the drill.

3.14 ENG PHYS Design Project

While working on this project, I supervised an Engineering Physics student group on a 4^{th} year design project related to the problem of measuring drilled bore depth in bone during surgery. They developed an alternative optical approach to measuring drill bit displacement, by shining a 'sheet' of light on or adjacent to the drill bit itself. A linear camera was directed so as to respond to light in a plane that intersected the sheet of projected light along a line. This camera would respond to the illuminated point where this intersection line encountered the bone (typically immediately adjacent to the drill bit). An image subtraction technique was used to continuously determine the depth of the drill bit, allowing drilled bore depth to be determined with a similar approach to that described above. Although the students presented

promising initial results, their prototype was not sufficiently developed to be evaluated in the experiments described in Chapter 4, though we believe that this technique could offer a lower-cost approach (as compared with laser range-finding) to achieving accurate bore depth measurement and we plan to evaluate their design in greater detail in future.

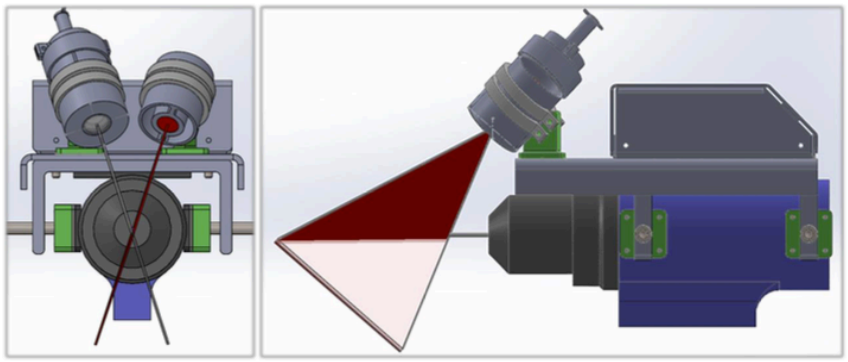

Figure 35 – ENG PHYS student design concept

3.15 Design Summary

The results for the pilot experiments for the different sensor concepts are presented in the next chapter. It is not a major limitation for a design to require a modified drill guide as they are commonly used in plastic and orthopedic surgery.

4 Materials and Methods

4.1 Overview

This chapter explains the experiments performed to assess the feasibility and reliability of a laser displacement sensor in developing a device for automatic measurement of drilled bore in bone during surgery. The concepts discussed in the Design chapter were tested in different animal models. Exploratory experiments were done to quickly assess the feasibility of the concepts, and are discussed here briefly. The concepts that performed best were assessed in the more formal Final Evaluation Experiments, which constitute most of the discussion.

4.2 Animal Models

I used different animal models at different phases of the project. They varied in terms of cost and surgical fidelity.

4.2.1 Chicken Long Bone

Initial tests were performed using chicken thighs obtained from the grocery store. The advantages of this model are low cost and convenience. The chicken femur is similar in size to the metacarpal bones of the human hand. Disadvantages of this model include the small size of the overall specimen compared with a human, and the relatively thin cortex of the avian long bone.

4.2.2 Porcine Long Bone

The porcine bone as a model has the advantages of being from a mammal of similar size and structure to humans. Porcine tissues are used in a range of surgical simulations (Swindle, Smith, and Hepburn 1988). The porcine femur has a similar diameter to that found in the

human. Experiments were done using bare porcine femurs obtained from a local butcher (Pete's Meats). These had the advantages of a similar bone quality to human long bones. However the total length of the specimen was significantly smaller than a human extremity. Additionally, the lack of surrounding soft tissues reduced the fidelity of the model in terms of how well it could simulate a typical surgical exposure.

Figure 36 - Porcine femur in drilling test

4.2.3 Porcine Hind Limb

On several occasions, I obtained total porcine hind limbs from a local butcher. I performed a surgical exposure of the femur and tibia to create a situation similar to a surgical approach on a human limb. The incision dimensions were also very close to those obtained from the dimensional analysis performed on orthopedic surgical exposures. This provided a high-fidelity animal model for orthopedic surgery of the appendicular skeleton.

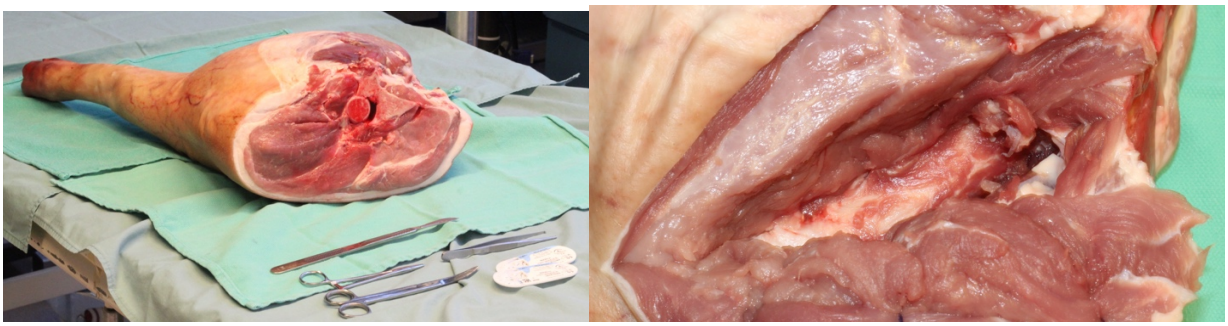

Figure 37 - Porcine hindlimb model

4.3 Exploratory Experiments

I performed a series of exploratory experiments to test first the feasibility and then the reliability of the different sensor configuration concepts described in the previous chapter. These pilot studies were all single user studies. The feasibility testing was done in the porcine bone model, and reliability testing in the porcine hindlimb model. A summary of the experiments and results is shown in Figure 39 and Table 4, with complete details are presented in Appendix D. Briefly, I drilled bicortical holes using the surgical drill with the attached sensor prototype, and computed drilled bore depth from the measured displacement traces using the method previously discussed (Chapter 3). I compared these values to those obtained using the conventional depth gauge and digital calipers, the latter of which served as the 'gold standard' for these experiments.

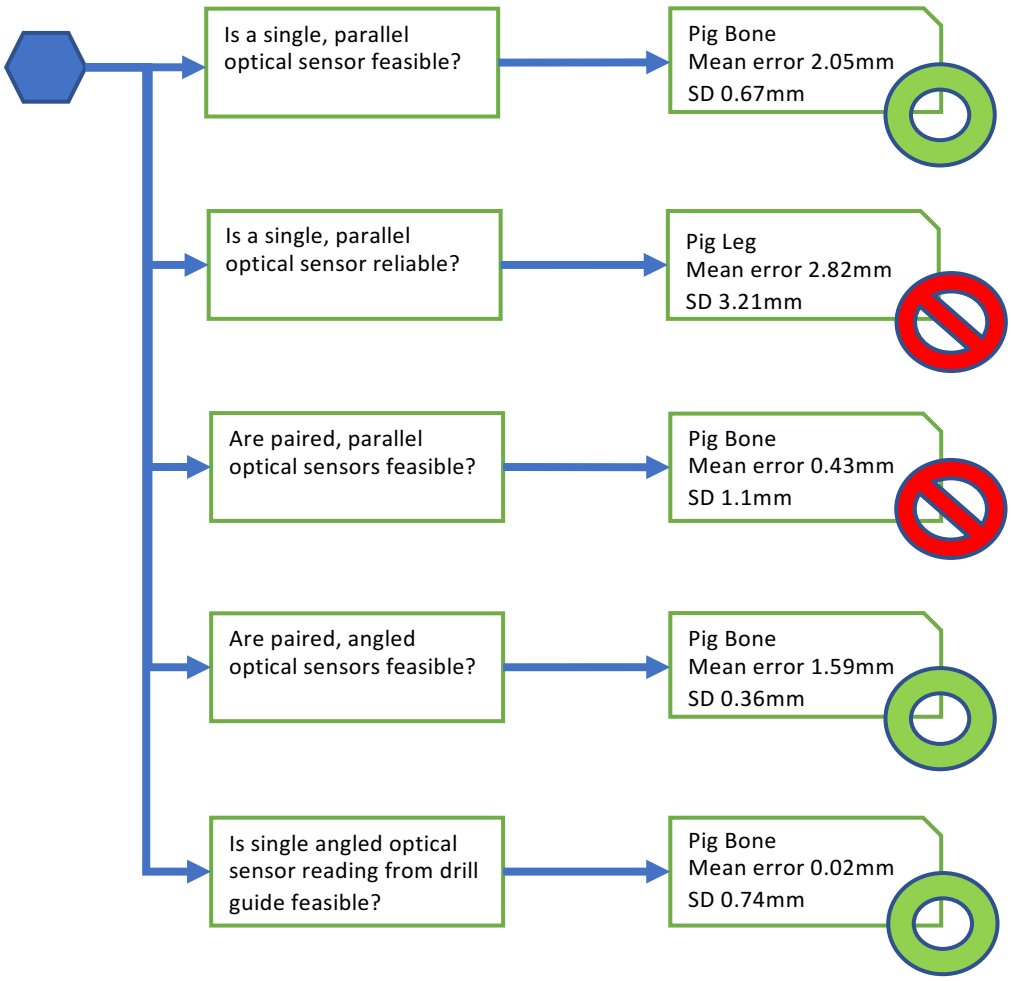

Figure 38 – Summary of exploratory experiments

Sensor Number, Orientation, Measurement target	single, parallel, tissue	single, parallel, tissue	dual, parallel, tissue	dual, angled, tissue	single, angled, drill guide
Animal Model	pig bone	pig leg	pig bone	pig bone	pig bone
n	9	25	20	7	11
Sensor Error (mm)	2.05	2.82	0.43	1.59	0.02
Sensor SD (mm)	0.67	3.21	1.1	0.36	0.74
Depth Gauge Error (mm)	1.55	0.71	-1.15	-0.69	-0.6
Depth Gauge SD (mm)	0.83	2.69	0.62	0.815	1.29

Table 4 – Results from exploratory experiments

As shown, most of the concepts resulted in a positive mean error from the gold standard bore depth measurement. This represents a bias in using this form of sensing (eg, potentially due to partial exiting of the drill bit prior to the breakthrough pulse happening) and could potentially be corrected for in the interpretation and/or computation step. More important is the variance of the error, which I took as the principal evaluation criterion. A discussion of the performance of each sensor arrangement and possible explanations are presented in Chapter 6. Based on these results, I decided to use both single and paired angled sensors reading from the drill guide in the final evaluation experiments.

4.4 Evaluation of Final Concept

Purpose: To evaluate the performance of the lead sensor concepts under a broader, more surgically relevant range of expected drilling conditions, with multiple surgeon users.

Designs Tested: 1) single angled laser displacement sensor measuring from mock drill guide and 2) dual angled laser displacement sensor measuring from mock drill guide.

Drilling conditions: information from the fixation construct analysis (see Needs Assessment) was used to select the drilling conditions for the experiment. Condition AM was not tested, as it is geometrically similar to SD and SM.

a. Condition SD - perpendicular diaphyseal drilling.
b. Condition SD - angled diaphyseal drilling.
c. Condition SM - perpendicular metaphyseal drilling.

Operators:

i. Daniel Demsey MD, plastic surgery resident (year 4 of training)
ii. Pierre Guy MD, staff orthopedic surgeon

Methods: All experiments were conducted in the Biomedical Engineering Laboratory at the Centre for Hip Health and Mobility located on the Vancouver General Hospital campus, part of the University of British Columbia. Appropriate specimen storage and handling protocols were followed at all times. Ethics approval was not required as only deceased animal tissue was used, and only members of the research team were involved in the experiments. Biosafety approval was obtained.

I used fresh porcine hind limbs for these experiments. In these experiments, I performed a surgical exposure of the femur and tibia of each hind limb specimen. I used suture ligature and muscle tissue removal to simulate appropriate retraction of tissues for bone exposure. I marked the transition between diaphysis and metaphysis with a marking pen for data collection, and placed the specimens on surgical drapes on a table at surgical working height. The LaserGauge prototype was mounted on a Conmed MPower2 surgical drill, a medium sized battery powered pistol type drill. I used 3.5mm diameter orthopedic surgical drill bits from Stryker in these experiments. The prototype sent data signals to an Arduino Due microprocessor, which transmitted data to a Matlab code run on a personal computer. Data files were saved for later analysis.

The experiment consisted of drilling a series of bicortical holes in the long bones (tibia and femur). Standard surgical technique was used. A piece of 1" thick aluminum with a predrilled hole the diameter of the drill bit was used to represent the drill guide. The drill bit was passed through the hole in the drill guide and seated on the bone, and then the drill guide was set flush against the bone surface with gentle pressure from the surgeon's non-dominant hand. The displacement sensors measured from the surface of the guide simulator. One

difference from normal surgical practice is that this approximation of a drill guide did not perform the normal function of stabilizing the drill entry point, as it did not have the metal 'teeth' present in a real drill guide.

The two surgeons alternated drilling the holes. The drilling condition of each hole to be drilled (SD, AD, or SM – see Figure 40) was selected in advance. Drilling conditions were evenly distributed between bone type (femur or tibia) and surgeon. After each hole was drilled the data plot was visually inspected to confirm an expected appearance based on previous experiments.

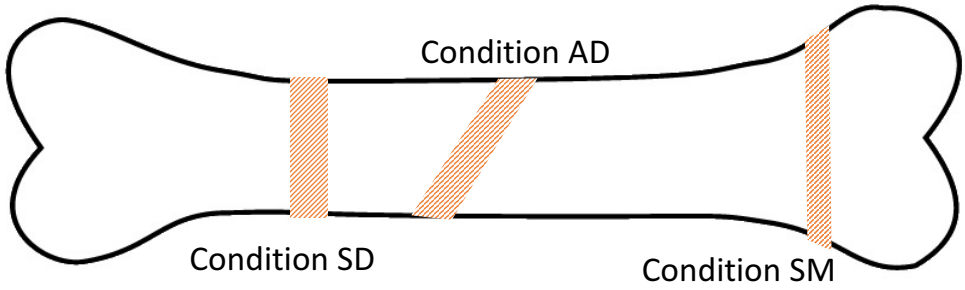

Figure 39 - Drilling conditions tested

Once all holes had been drilled, I measured the depth of each hole using the conventional depth gauge. It was used in the usual fashion, and if three attempts failed to obtain a measurement, the value was recorded as a 'failure'. Measurements were recorded in an Excel spreadsheet. After these measurements were obtained I dissected the long bones free from the soft tissues. I then used digital calipers to measure the hole depth. Specimens were then sealed in plastic for CT imaging. The bones were imaged using High Resolution Peripheral Quantitative Computer Tomography (HR-pqCT) in an XTreme-CT model device (Sanco). Two bones were imaged at once to save costs. Image files were saved in DICOM format and loaded into MIMICS software (Materialise, Belgium) for analysis. The entry and exit points of each hole

were identified in the CT volumes twice on the proximal and distal aspect of the bore and the results averaged to produce the final 'gold standard' value of hole depth.

A total of 125 drilling attempts were made in 4 porcine hindlimbs. 95 holes were suitable for analysis, with 30 holes rejected for the following reasons: overlap with adjacent holes (n=3), drill bit exit into joint space (n=11), technical problems with the drill (drill bit loosening or drained battery) (n=3), and technical problems with the prototype apparatus (clamp coming loose, sensor shifting relative to drill)(n=13). Of the 95 holes included in the analysis, 28 holes were from Condition SD, 22 holes from Condition AD, and 36 holes from condition SM. Each drilled hole depth was analyzed using both a single sensor reading and the dual sensor reading.

5 Results

5.1 Overview

This chapter presents the results of the Final Evaluation experiments, which evaluated the dual angled laser sensor design measuring from a drill guide, and then discusses the interpretation of the results, along with implications for clinical application.

5.2 Final Evaluation Results

Mean errors and standard deviations for the two sensors treated individually as well as in combination are shown in Table 5, separated by user and drilling condition. The combined sensor tended to have less variability than either sensor individually, and was more consistent than either sensor individually across the multiple tests. However, each single sensor met the design criteria of having less variability than the conventional depth gauge under all drilling conditions. A positive bias in the measurement (ie, over-estimation of hole depth) was present. An explanation for the bias could be that the tip of the drill emerges from the bone prior to the edges of the cortex giving way and allowing the bit to plunge through, resulting in a 'delay' of the acceleration spike. Curiously, the reading from sensor 1 seemed to be consistently more biased than that from sensor 2 across all conditions and users, which is not directly compatible with the above hypothesis.

	User 1 (DD)				User 2 (PG)			
	Sensor 1	Sensor 2	Combined	Depth Gauge	Sensor 1	Sensor 2	Combined	Depth Gauge
Condition SD								
Mean Error (mm)	2.56	0.10	1.33	0.10	2.72	-0.01	1.36	-0.28
SD	0.65	0.81	0.66	1.16	0.88	0.77	0.78	1.66
n	16	16	16	16	12	12	12	12
Condition AD								
Mean Error (mm)	2.77	0.37	1.57	1.68	3.01	0.48	1.74	3.04
SD	0.86	1.05	0.87	4.49	0.78	1.07	0.87	3.00
n	11	11	11	10	11	11	11	10
Condition SM								
Mean Error (mm)	3.49	0.33	1.91	1.01	3.65	0.91	2.28	1.91
SD	0.97	0.84	0.75	3.06	1.31	1.16	0.81	3.34
n	16	16	16	14	20	20	20	16

Table 5– Final evaluation data summary

In terms of variability, the data from the two sensors treated individually is relatively similar to one another, so for the balance of our analysis, we consider only the data for the combined sensors. Statistical comparison of the variability between users for each drilling condition showed no significant differences (F test for unequal variances, $p<0.05$). Based on this, the data for the two users was combined and is presented in Table 6.

	Dual Laser Sensor	Depth Gauge	Statistically Significant
Condition SD			
Mean error (mm)	1.34	-0.06	
SD (mm)	0.70	1.38	*
n	28	28	
Condition AD			
Mean error (mm)	1.66	2.36	
SD (mm)	0.86	3.79	*
n	22	20	
Condition SM			
Mean error (mm)	2.11	1.51	
SD (mm)	0.80	3.19	*
n	36	30	

Table 6 – Mean error and SD for the dual laser prototype compared with conventional depth

I compared the variances for each drilling condition using the dual laser sensor and the depth gauge and found the laser sensor to have significantly less variability under all conditions (F test for unequal variance, $p<0.05$). Interestingly, the depth gauge showed markedly higher variability for the two conditions with angles on either or both of the entry and exit points, whereas there was no noticeable difference amongst these conditions for the laser-based sensor.

The mean error for the prototype and the conventional method is shown graphically in Cumulative Frequency Distribution and Bland Altman plots below. Detailed experimental results are present in Appendix E.

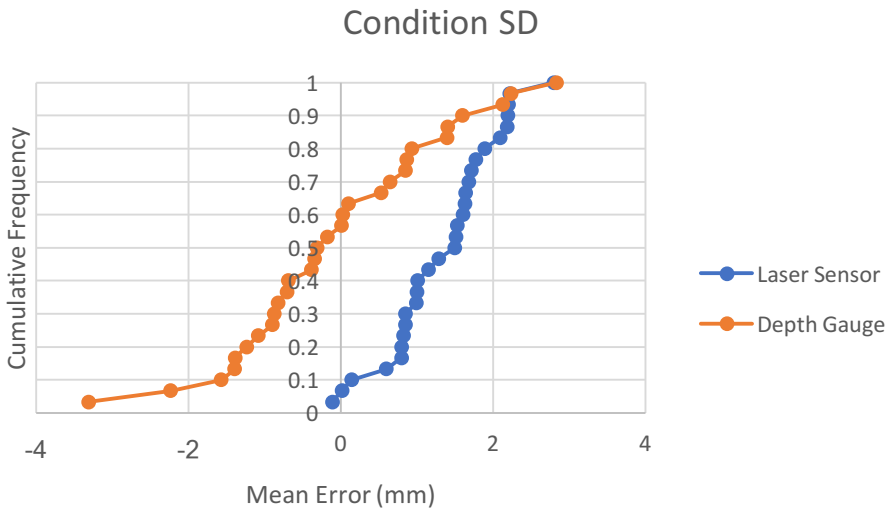

Figure 40 - Cumulative frequency distribution for Condition SD

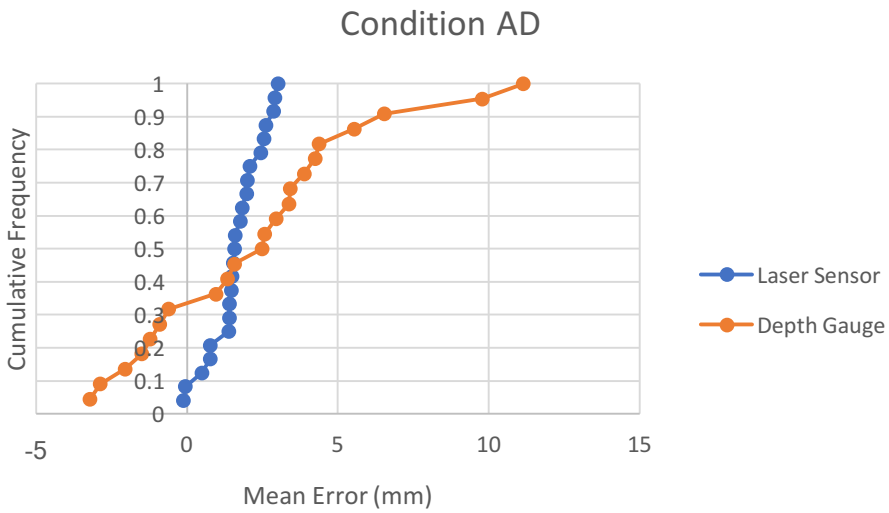

Figure 41 - Cumulative frequency distribution for Condition AD

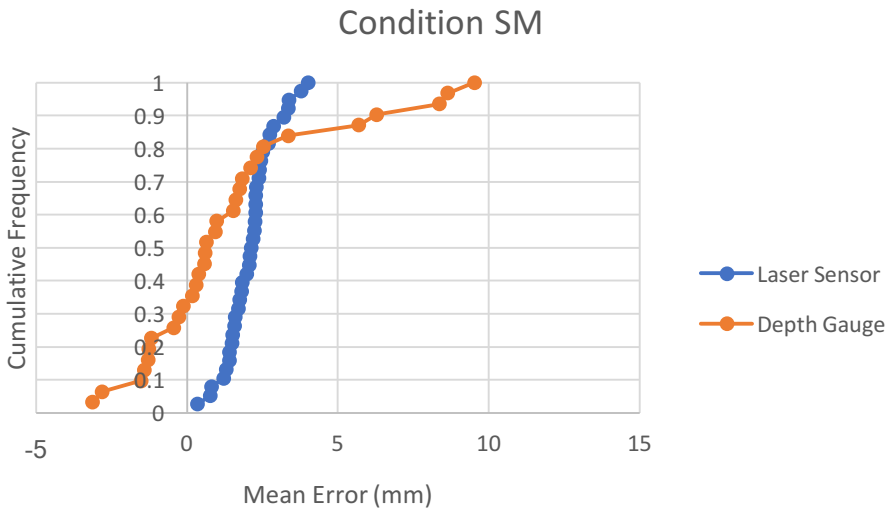

Figure 42 - Cumulative frequency distribution for Condition SM

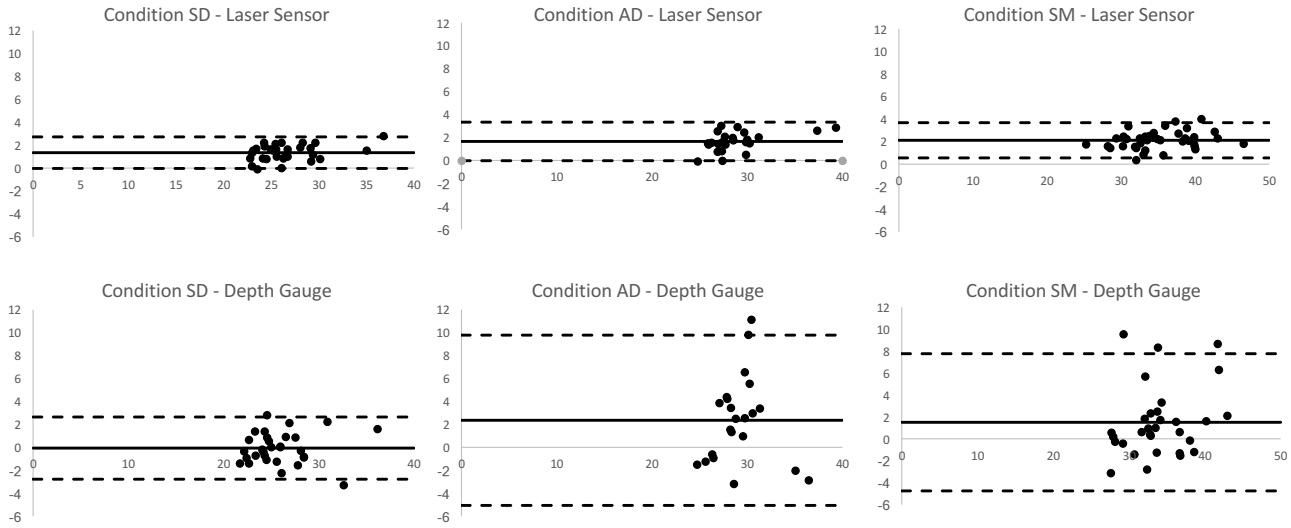

Figure 43 – Bland Altman plots for the LaserGauge and the conventional depth gauge comparing to CT scan as 'gold standard'

The Cumulative Frequency Distribution and Bland Altman plots demonstrate that there was a notable positive bias in the measurements made by the LaserGauge, and a significantly lower variability in mean error than the conventional gauge (including condition SD).

6 Discussion

6.1 Significance of Design

Using an optical sensor mounted on an existing surgical drill to measure bore depth in bone has not been previously described in the literature. Drills with automatic bore depth measurement capabilities have been described, but all require replacement of the existing drill hand piece(Louredo, Díaz, and Gil 2012; Ong and Bouazza-Marouf 1998; Benedetto Allotta, Giacalone, and Rinaldi 1997; Wen-Yo Lee and Shih 2006). The advantage of our approach is that it requires minimal change from existing surgical practice and uses existing surgical equipment. I have demonstrated that a design using laser triangulation is feasible in multiple forms, and that a paired sensor device measuring from a modified drill guide more reliable than the conventional depth gauge in the laboratory setting.

6.2 Sensor Concepts

6.2.1 Single vs. Dual Sensors

The single, parallel sensor performed better than the conventional depth gauge in the feasibility testing in pig bone models (mean error 2.05mm SD 0.67mm vs mean error 0.83mm SD 1.55mm), providing an initial indication that the optical sensor concept could potentially work for automatic measurement of drilled bore in bone under sufficiently controlled conditions. However, it did not perform as well in the reliability testing compared with the conventional method in the more realistic pig leg model (mean error 2.82mm SD 3.21mm vs. 0.71mm SD 2.69mm).

Using a single sensor reading from tissue relies on an assumption of perfect (or near perfect) forward motion of the drill along the drilling axis. In surgery, the drill is used free-hand so this may not be a valid assumption. The effect of the drill tilting about the contact point of the drill bit on the bone is shown in Figure 45, and may be a source of the error found in the feasibility testing. Depending on the direction the drill tilts, the measured displacement of the sensor from the bone will increase or decrease without any progress in bore drilling, resulting in inaccuracies in the final computed bore depth (a change in indicated displacement not due to drilling).

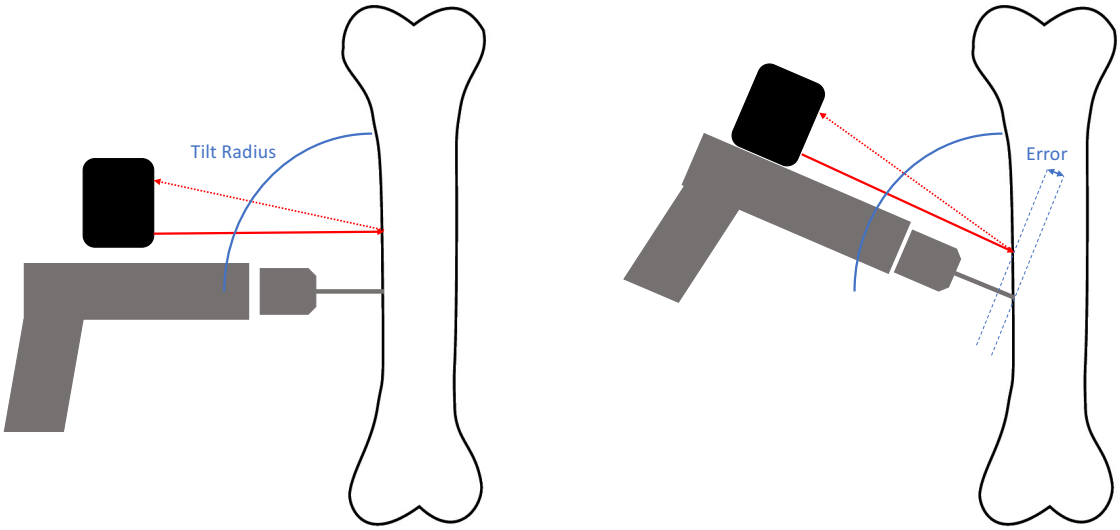

Figure 44 – Effect of drill tilt on sensor readings

The orientation of the drill could also change once the first cortex is breached, as the medulla is essentially hollow and does not present significant resistance to movement of the drill bit perpendicular to the drilling axis. This is shown in Figure 46. The resulting effect on displacement measurement is similar to that seen in the 'tilt' phenomenon described above.

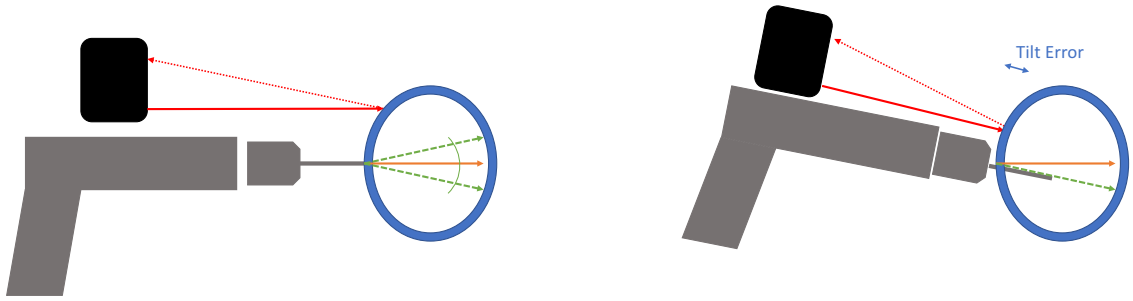

Figure 45 – Effect of change of drill trajectory on sensor readings

The drill vibrates during operation, and this could result in movement in a radial direction about the drilling axis. As the surface of the tissue is not flat, this will again result in changes in measured displacement not associated with forward drill movement and error in the computed bore depth (see Figure 47).

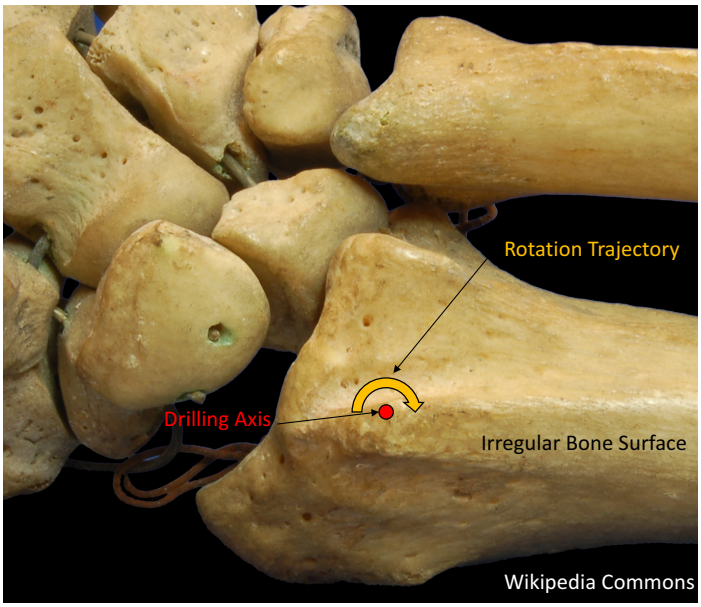

Figure 46 – Rotation and irregular bone surface

The addition of a second sensor on the opposite side of the drilling axis and averaging the bore depths computed with each sensor individually should reduce the effect of these errors. Generally, tilt resulting in a decrease in one displacement measurement should result in an equal increase in displacement measurement in the sensor on the opposite side, and vice

versa. This is shown in Figure 48. Errors associated with rotational movement of the drill are likely to decrease due to statistical effects of multiple measurements (regression to mean).

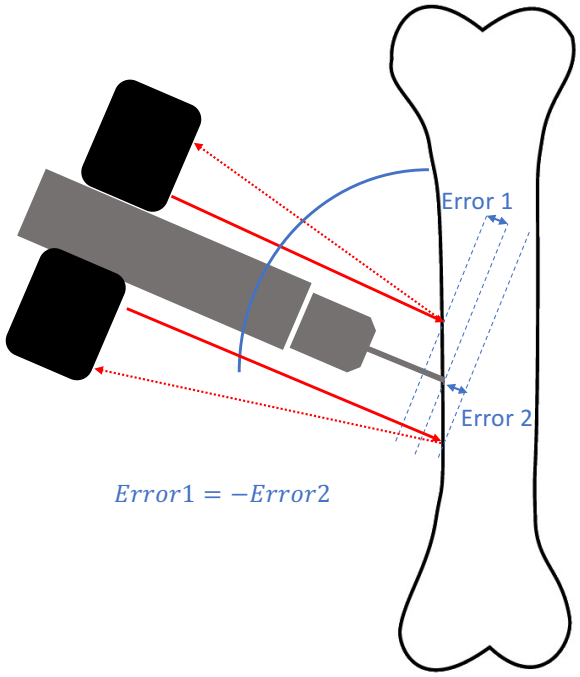

Figure 47 - Two sensors on opposite sides of drilling axis correct for tilt error

6.2.2 Parallel vs. Angled Sensors

Placing the sensor in a collinear orientation to the drilling axis leads to a simple design and doesn't require mathematical correction of the measured displacement. However, given the geometry of the drill and mounting system, there is a limit to how much the offset between the drilling axis and the sensor beam can be reduced. In my prototypes, the minimum offset is approximately 3 cm. Reducing this distance would reduce the effect of tilt error described above.

By angling the sensor towards the drilling axis, the distance between the point of drilling and the point from which displacement can be measured is reduced. Implementing this change

in the prototype design improved the performance relative to the collinear sensor (mean error 1.59mm SD 0.36mm vs. 0.43mm SD 1.1mm). There were not enough data points for this difference to reach statistical significance.

6.2.3 Tissue vs. Drill Guide Reference

Drill guides are routinely used in surgical practice to allow for better control of the drill bit trajectory("Oxford Textbook of Trauma and Orthopaedics - Oxford Medicine" 2017). Adding a feature with a machined, uniform surface could improve the performance of the prototype in multiple ways. First, the uniform surface would prevent errors due to rotational vibration of the drill, as slight rotational movements of the measured point would not significantly change the measured displacement. Second, the orientation of the drill bit would be constrained relative to the drill guide (Figure 49) so that tilt or movement of the drill perpendicular to the drilling axis would not be possible. This would prevent the tilt-associated error described above.

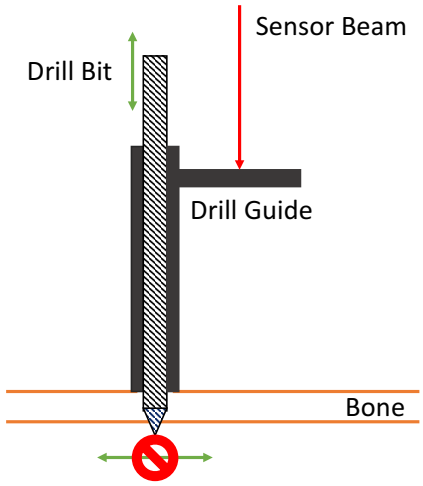

Figure 48 – Drill guide constraints

6.3 Drilling Conditions

6.3.1 Condition SD

The conventional depth gauge performed best in the SD condition when compared with the other conditions. This is intuitive as the depth gauge should obtain the same measurement regardless of which position around the circumference of the hole it hooks to.

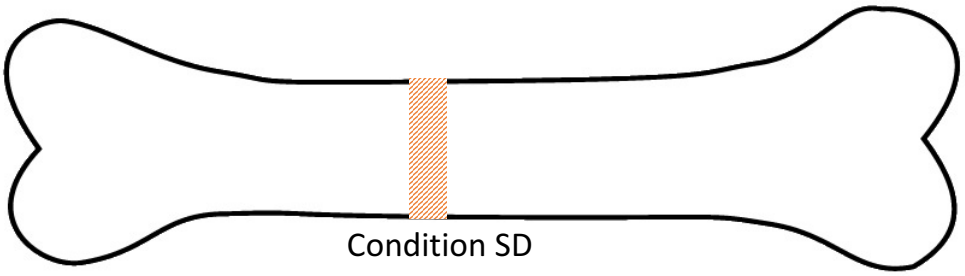

Figure 49 - Condition SD

6.3.2 Condition AD

The greatest discrepancy between prototype and conventional depth gauge was when drilling in Condition AD. The prototype performed significantly better under these conditions. The angled bore does not allow for perpendicular contact of the gauge against the bone cortex which could explain the accuracy issues. It could also be due to variations in the measured value depending on which side of the bone the instrument engages with.

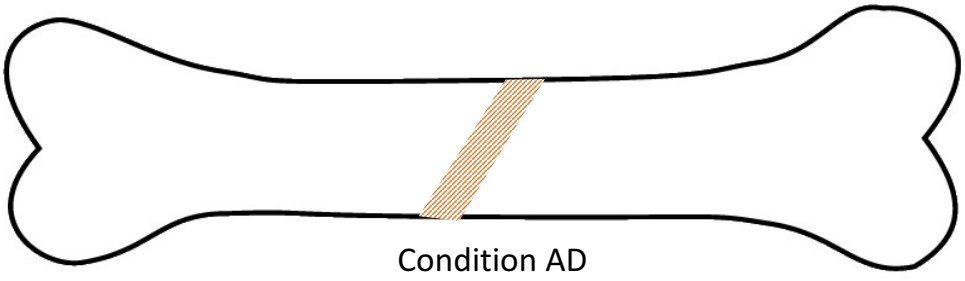

Figure 50 - Condition AD

6.3.3 Condition SM

The measurements made by the conventional depth gauge also showed significant variability in the straight metaphyseal condition. The prototype showed consistent performance with the other conditions.

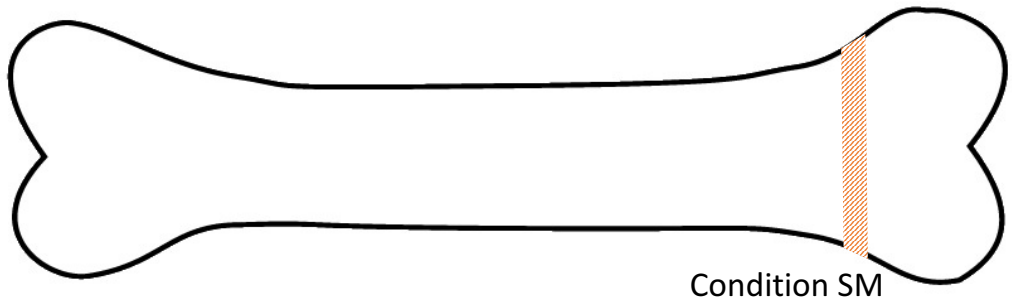

Figure 51 - Condition SM

6.4 Final Concept Selection

Based on the experimental results, an angled beam measuring from the drill guide surface performed the best. Two sensors had better performance than one, but the single sensor still functioned better than the conventional depth gauge. Based on the results presented here, our recommended design is the angled dual sensor measuring from the drill guide. However, depending on final design costs, a single sensor version could be acceptable based on experimental results.

6.5 Bore Depth 'Gold Standard'

6.5.1 Bone Geometry

Animal and human bones have an irregular geometry, making the definition of 'true' bore depth difficult to define or measure. The measurement can vary depending on whether it

is taken at the sides of the drilled bore or the centroid. This is shown in Figure 53. The three arrows show different 'depths' of the bore when measured at different points.

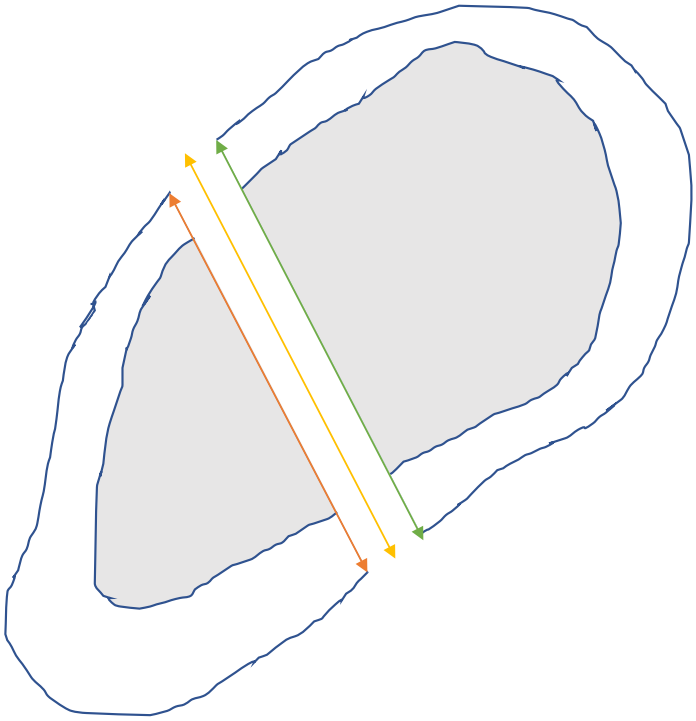

Figure 52 – Measurement variations in bone bore, shown in cross section. Three arrows indicated three different measurements of bore depth.

6.5.2 Measurement Methods

For the purposes of my experiments we used a CT scan based 'gold standard' measurement of the drilled bore depth in the final evaluation. To obtain this, I performed high resolution CT scan of the bones after drilling, and measured the depth of the drilled bore from the 3D reconstructions in MIMICS software. The measurement of the bore was taken on two sides of the drilled bore, and an average was taken of these two values to give the 'gold standard' value. In Figure 53 this would be the average of the orange and the green measurement. Significant differences were noted between the measurements of depth on the opposing side of the bore on the CT scan (mean difference 0.46mm, SD 1.42mm). Averaging

these values would logically produce a closer estimate of the true bore depth, but this also emphasizes the intrinsic ambiguity as to what is the 'true' depth of the drilled bore.

6.5.3 Interpretation of Measurement by Surgeon

The significance of the bore depth measurement is the effect it has on the choice of screw length. Choosing a longer screw means a better chance of full thread engagement in all the available cortical bone, resulting in a stronger fixation construct. However, this means a greater chance of the screw extending beyond the far bone cortex and potentially impinging on and damaging adjacent sensitive structures. Choosing a shorter screw lowers this chance but also is more likely to result in weaker fixation construct.

In an interview, Dr. Guy, a staff orthopedic surgeon, stated that the interpretation of the measurement and resulting screw selection depends highly on the anatomic location. The surgeon will choose a shorter screw in areas where complications of long screws are frequent such as the distal radius.

6.5.4 Required Precision

For evaluation purposes I set an initial target precision of +/- 1 mm relative to true bore depth. As I performed the evaluation experiments it became apparent that there was uncertainty as to what is the true 'gold standard' for bore depth, and that the conventional depth gauge, which has a clinically accepted precision, was not close to meeting my original target. The criteria for acceptable performance was then revised to be less variance in repeated measurement than the conventional gauge. Only in the smallest sizes (<10 mm length) of screws is a precision of 1 mm clinically necessary, as small screws increase in size by an increment of 1 mm. In screws > 10 mm in length, the increments become 3 mm and then 5

mm, making measurement precision less critical. Testing in a more representative simulation, with placement of screws based on the bore depths estimated by our device could better delineate the clinical precision sensitivity. Exceeding the performance of the current instrument is a reasonable indication of design success.

6.6 Additional Considerations

Medical devices require FDA approval prior to use. Devices are classified based on the risk they present to patients, and the regulatory pathway varies for the different classes (Health 2017). The cost difference between the regulatory pathways is considerable, and so it can be an important design consideration to target a specific regulatory pathway. The LaserGauge is likely to be identified as a Class II device, and the ideal regulatory process would be through the 510(k) Exception. This would be an important factor moving forward with the design.

6.7 Existing Literature

The published engineering and medical literature do not, to my knowledge, contain any research focused on the methods of measuring bore depth in bone during surgery. This has been a considered a solved problem for some time, so it is understandable that this has not been looked at rigorously prior to our work.

6.8 Limitations

Limitations of my experimental work include being performed in deceased animal tissue, which could have somewhat different mechanical properties than live human tissue and thereby affect the breakthrough dynamics, though we regard this as relatively unlikely. In the current version of the system, the measurements required post-processing to determine a bore

depth and were done using a process that involved human interaction rather than an automatic algorithm; such an automatic analysis technique would be required to implement a clinically-usable device. Finally, the measurements were not used to select screw length for a fixation construct, so the rate of incorrect screw placement could not be compared between our device and the conventional depth gauge.

7 Conclusion

My research objective was to determine whether optical displacement sensors could be used to measure drilled bore depth in bone during surgery. I was able to show that this concept is feasible and reliable in a simulated surgical setting. A prototype based on two laser displacement sensors, angled towards the drilling axis and measuring from a custom drill guide, displayed markedly less variability in measurement error than the conventional depth gauge in a range of clinically relevant simulated drilling conditions.

The problem of measuring drilled bore depth during surgery was identified by practicing surgeons, and the solution has been developed with them and their patients in mind. This approach has not been previously described in the published academic literature. There is a patent for a similar concept, and we have spoken with a research group (AO) that is developing a similar idea. However neither of these groups have described successful validation of their design, nor have they explored the range of optical sensor arrangements described in this thesis. A device using this concept has the potential to improve current surgical practice, resulting in fewer complications secondary to incorrect size screw placement. It could also significantly improve the user experience for practicing surgeons.

7.1 Future Work

Multiple design milestones must be achieved prior to completion of a 'works like' prototype.

In the first stage, the device must be made to function automatically and in a stand-alone configuration. To do this, an algorithm needs to be developed and tested to automatically determine the drilled bore depth without user interpretation at the post

processing phase. This algorithm may be developed in MATLAB, but ultimately must be converted to C++ or a similar language to run on the prototype's microprocessor. A user interface with displays and controls is also required. Lastly, the prototype must also be converted to a battery-based power supply.

A drill guide with a feature to support displacement measurement must be designed and produced, and must ultimately be compatible with a range of drill bit diameters. This would likely be done with a single guide with exchangeable 'sizing' components.

After the 'works-like' prototype is complete, a usability test would be performed in both animal and cadaver tissue. A screw and plate fixation construct would be placed using the device's measurements, and afterwards the adequacy of the construct would be assessed, likely both by mechanical loading and by inspection following dissection. User experience metrics would also be analyzed through a post-use survey. If indications are strongly positive at this point, we would likely begin consultations with potential commercialization partners.

In order to move forward to a clinical testing phase, a housing and sterilization protocol would also need to be developed. This is an expensive step that would involve contracting a third-party organization to validate the sterilization protocol. The main challenge is likely to be how to protect the sensitive electronic components from the harsh sterilization conditions (see Appendix F).

Once a sterilizable 'works like' prototype has been produced, we would be in a position to conduct a clinical use study and ultimately to learn how effective our LaserGauge device would be in clinical practice.

References

Aerssens, Jeroen, Steven Boonen, Geert Lowet, and Jan Dequeker. 1998. “Interspecies Differences in Bone Composition, Density, and Quality: Potential Implications for in Vivo Bone Research.” *Endocrinology* 139 (2): 663–70. doi:10.1210/endo.139.2.5751.

Allotta, B., F. Belmonte, L. Bosio, and P. Dario. 1996. “Study on a Mechatronic Tool for Drilling in the Osteosynthesis of Long Bones: Tool/Bone Interaction, Modeling and Experiments.” *Mechatronics*, Mechatronics in Surgery, 6 (4): 447–59. doi:10.1016/0957-4158(96)00005-0.

Allotta, Benedetto, Giuseppe Giacalone, and Luigi Rinaldi. 1997. “A Hand-Held Drilling Tool for Orthopedic Surgery.” *IEEE/ASME Transactions on Mechatronics* 2 (4): 218–229.

Basiaga, Marcin, Zbigniew Paszenda, and Janusz Szewczenko. 2010. “Biomechanical Behaviour of Surgical Drills in Simulated Conditions of Drilling in a Bone.” In *Information Technologies in Biomedicine*, 473–81. Springer, Berlin, Heidelberg. doi:10.1007/978-3-642-13105-9_48.

Berkovic, Garry, and Ehud Shafir. 2012. “Optical Methods for Distance and Displacement Measurements.” *Advances in Optics and Photonics* 4 (4): 441. doi:10.1364/AOP.4.000441.

Brett, P. N., D. A. Baker, L. Reyes, and J. Blanshard. 1995. “An Automatic Technique for Micro-Drilling a Stapedotomy in the Flexible Stapes Footplate.” *Proceedings of the Institution of Mechanical Engineers, Part H: Journal of Engineering in Medicine* 209 (4): 255–262.

Carter, Dennis R., Greg H. Schwab, and Dan M. Spengler. 1980. “Tensile Fracture of Cancellous Bone.” *Acta Orthopaedica Scandinavica* 51 (1–6): 733–41. doi:10.3109/17453678008990868.

Caruso, Giancarlo, Andrea Vitali, and Ferdinando del Prete. 2015. “Multiple Ruptures of the Extensor Tendons after Volar Fixation for Distal Radius Fracture: A Case Report.” *Injury* 46: S23–27. doi:10.1016/S0020-1383(15)30040-1.

Cavers, Andrew, Juan Pablo Gomez, Sebastian Munoz, Alex Seal, and Antony Hodgson. 2016. “Improved Drill Hole Depth Measurement in Fracture Fixation.” In *16th Annual Meeting of the International Society for Computer Assisted Orthopaedic Surgery*. Osaka, Japan.

Colla, Valentina, and Benedetto Allotta. 1998. “Wavelet-Based Control of Penetration in a Mechatronic Drill for Orthopaedic Surgery.” In *Robotics and Automation, 1998. Proceedings. 1998 IEEE International Conference on*, 1:711–716. IEEE. http://ieeexplore.ieee.org/abstract/document/677057/.

Colton, Chris, Steve Krikler, Joseph Schatzker, Peter Trafton, and Richard Buckley. 2017. “AO Foundation Surgery Reference.” Accessed May 3. https://www2.aofoundation.org/wps/portal/surgery.

Coulson, C. J., M. Zoka Assadi, R. P. Taylor, X. Du, P. N. Brett, A. P. Reid, and D. W. Proops. 2013. “A Smart Micro-Drill for Cochleostomy Formation: A Comparison of Cochlear Disturbances with Manual Drilling and a Human Trial.” *Cochlear Implants International* 14 (2): 98–106. doi:10.1179/1754762811Y.0000000018.

Gunther, Walter A., and Edward J. Keyes. 1948. “A Depth Gauge for Bone Surgery.” *J Bone Joint Surg Am* 30 (1): 233–233.

Health, Center for Devices and Radiological. 2017. “Overview of Device Regulation.” WebContent. Accessed May 24. https://www.fda.gov/MedicalDevices/DeviceRegulationandGuidance/Overview/ucm200530 0.htm.

Hsu, Yeh-Liang, Shih-Tseng Lee, and Hao-Wei Lin. 2001. “A MODULAR MECHATRONIC SYSTEM FOR AUTOMATIC BONE DRILLING.” *Biomedical Engineering: Applications, Basis and Communications* 13 (4): 168–74. doi:10.4015/S1016237201000212.

“IntelliSense Bone Drill With Auto Depth Measurement and Edge Detection FDA Cleared (VIDEO) |.” 2015. *Medgadget*. March 2. https://www.medgadget.com/2015/03/intellisense-bone-drill-with-auto-depth-measurement-and-edge-detection-fda-cleared-video.html.

Lee, Wen-Yo, and Ching-Long Shih. 2006. “Control and Breakthrough Detection of a Three-Axis Robotic Bone Drilling System.” *Mechatronics* 16 (2): 73–84. doi:10.1016/j.mechatronics.2005.11.002.

Lee, W.-Y., C.-L. Shih, and S.-T. Lee. 2004. “Force Control and Breakthrough Detection of a Bone-Drilling System.” *IEEE/ASME Transactions on Mechatronics* 9 (1): 20–29. doi:10.1109/TMECH.2004.823850.

Leong, J. J. H., D. R. Leff, A. Das, R. Aggarwal, P. Reilly, H. D. E. Atkinson, R. J. Emery, and A. W. Darzi. 2008. “Validation of Orthopaedic Bench Models for Trauma Surgery.” *Bone & Joint Journal* 90–B (7): 958–65. doi:10.1302/0301-620X.90B7.20230.

Louredo, Marcos, Iñaki Díaz, and Jorge Juan Gil. 2012. “DRIBON: A Mechatronic Bone Drilling Tool.” *Mechatronics* 22 (8): 1060–1066.

Louredo, Marcos, Inaki Diaz, and Jorge Juan Gil. 2012. “A Robotic Bone Drilling Methodology Based on Position Measurements.” In , 1155–60. IEEE. doi:10.1109/BioRob.2012.6290304.

Maschke, Steven D., Peter J. Evans, David Schub, Richard Drake, and Jeffrey N. Lawton. 2007. “Radiographic Evaluation of Dorsal Screw Penetration After Volar Fixed-Angle Plating of the Distal Radius: A Cadaveric Study.” *HAND* 2 (3): 144–50. doi:10.1007/s11552-007-9038-2.

Matityahu, Amir, Christof Hurschler, Markus Badenhop, Christina Stukenborg-Colsman, Hazibullah Waizy, Brock Wentz, Meir Marmor, and Christian Krettek. 2013. “Reduction of Pullout Strength Caused by Reinsertion of 3.5-Mm Cortical Screws.” *Journal of Orthopaedic Trauma* 27 (3): 170–176.

Mattos e Dinato, Mauro César, Márcio de Faria Freitas, and Alexandre Sadao Iutaka. 2010. “A Porcine Model For Arthroscopy.” *Foot & Ankle International* 31 (2): 179–81. doi:10.3113/FAI.2010.0179.

Netter, Frank H. 2014. *Atlas of Human Anatomy E-Book*. Elsevier Health Sciences.

Ong, Fook Rhu, and Kaddour Bouazza-Marouf. 1998. “Drilling of Bone: A Robust Automatic Method for the Detection of Drill Bit Break-Through.” *Proceedings of the Institution of Mechanical Engineers, Part H: Journal of Engineering in Medicine* 212 (3): 209–221.

“Oxford Textbook of Trauma and Orthopaedics - Oxford Medicine.” 2017. Accessed January 13. http://oxfordmedicine.com/view/10.1093/med/9780199550647.001.0001/med-9780199550647.

Ozer, Kagan, and Serdar Toker. 2011. “Dorsal Tangential View of the Wrist to Detect Screw Penetration to the Dorsal Cortex of the Distal Radius after Volar Fixed-Angle Plating.” *Hand (New York, N.Y.)* 6 (2): 190–93. doi:10.1007/s11552-010-9316-2.

Qi, Lin, Xiaona Wang, and Max Q. Meng. 2014. “3D Finite Element Modeling and Analysis of Dynamic Force in Bone Drilling for Orthopedic Surgery: 3D FEA OF BONE DRILLING FOR ORTHOPEDIC SURGERY.” *International Journal for Numerical Methods in Biomedical Engineering* 30 (9): 845–56. doi:10.1002/cnm.2631.

Quest, D., C. Gayer, and P. Hering. 2012. “Depth Measurements of Drilled Holes in Bone by Laser Triangulation for the Field of Oral Implantology.” *Journal of Applied Physics* 111 (1): 13106. doi:10.1063/1.3676219.

Reilly, Donald T., and Albert H. Burstein. 1975. “The Elastic and Ultimate Properties of Compact Bone Tissue.” *Journal of Biomechanics* 8 (6): 393IN9397–396IN11405.

Rho, Jae-Young, Liisa Kuhn-Spearing, and Peter Zioupos. 1998. “Mechanical Properties and the Hierarchical Structure of Bone.” *Medical Engineering & Physics* 20 (2): 92–102.

Schnur, D. P., and B. Chang. 2000. “Extensor Tendon Rupture after Internal Fixation of a Distal Radius Fracture Using a Dorsally Placed AO/ASIF Titanium Pi Plate. Arbeitsgemeinschaft Für Osteosynthesefragen/Association for the Study of Internal Fixation.” *Annals of Plastic Surgery* 44 (5): 564–66.

“Smart Drill – Prevent Plunge, Measure and Control Depth, Determine Bone Density.” 2017. Accessed May 1. http://www.smartmeddevices.com/.

Smith, A. M., J. A. Forder, S. R. Annapureddy, K. S. K. Reddy, and A. A. Amis. 2005. “The Porcine Forelimb as a Model for Human Flexor Tendon Surgery.” *Journal of Hand Surgery* 30 (3): 307–309.

Swindle, M. Michael, Alison C. Smith, and Bradley J. S. Hepburn. 1988. “Swine as Models in Experimental Surgery.” *Journal of Investigative Surgery* 1 (1): 65–79. doi:10.3109/08941938809141077.

Taylor, R, X Du, D Proops, A Reid, C Coulson, and P N Brett. 2010. “A Sensory-Guided Surgical Micro-Drill.” *Proceedings of the Institution of Mechanical Engineers, Part C: Journal of Mechanical Engineering Science* 224 (7): 1531–37. doi:10.1243/09544062JMES1933.

Tuijthof, G.J.M., C. Frühwirt, and C. Kment. 2013. “Influence of Tool Geometry on Drilling Performance of Cortical and Trabecular Bone.” *Medical Engineering & Physics* 35 (8): 1165–72. doi:10.1016/j.medengphy.2012.12.004.

Winter, David A., H. Grant Sidwall, and Douglas A. Hobson. 1974. “Measurement and Reduction of Noise in Kinematics of Locomotion.” *Journal of Biomechanics* 7 (2): 157–59. doi:10.1016/0021-9290(74)90056-6.

Appendix A – Incision Dimensional Analysis

A.1 Overview

This appendix contains the data tables for the Incision Dimensional Analysis. This information came from analysis of the images from the textbook '*Atlas of Surgical Exposures of the Upper and Lower Extremity*' by Tubiana et call (Martin Dunitz Ltd. 2000). Reference measurements were performed on a human volunteer.

A.2 Data Tables

Surgical Exposure Dimensional Analysis

n=29	Image (Dimensionless)				Human (measured)		*predicted		
Image	IncisionL	Incision W	BoneL	BoneW	**refIncision**	**correctionF**	IncisionW*	BoneL*	BoneW*
Femur1	14.5	4.9	8.1	1.2	30	2.068965517	10.13793103	16.75862069	2.482758621
Femur2	12	7	6.6	1.6	26	2.166666667	15.16666667	14.3	3.466666667
Femur3	11.7	7.3	7	1.8	20	1.709401709	12.47863248	11.96581197	3.076923077
Femur4	12.7	5.5	6.8	1.2	23	1.811023622	9.960629921	12.31496063	2.173228346
Femur5	12.5	5.4	6.4	1.2	18	1.44	7.776	9.216	1.728
Femur6	12.6	6.8	4.7	1	22	1.746031746	11.87301587	8.206349206	1.746031746
Fibula1	11.6	5.5	7.8	0.5	16	1.379310345	7.586206897	10.75862069	0.689655172
Fibula2	13.6	4	9	0.5	16	1.176470588	4.705882353	10.58823529	0.588235294
Fibula3	13.3	6	8.1	1	18	1.353383459	8.120300752	10.96240602	1.353383459
Humerus1	9.8	5.1	5.7	0.9	15	1.530612245	7.806122449	8.724489796	1.37755102
Humerus2	7.7	4.9	4.4	1	27	3.506493506	17.18181818	15.42857143	3.506493506
Humerus3	8.1	5.5	5.9	1.2	10	1.234567901	6.790123457	7.283950617	1.481481481
Humerus4	7.8	5.6	5.9	1.4	12	1.538461538	8.615384615	9.076923077	2.153846154
Humerus5	10.8	4.7	6.9	1.2	20	1.851851852	8.703703704	12.77777778	2.222222222
Humerus6	8.1	5.3	4.9	0.8	25	3.086419753	16.35802469	15.12345679	2.469135802
Humerus7	9.9	4.2	3.9	1.1	18	1.818181818	7.636363636	7.090909091	2
Radius1	12	4.8	10.4	1	16	1.333333333	6.4	13.86666667	1.333333333
Radius2	7.5	3.5	3.9	1	12	1.6	5.6	6.24	1.6
Radius3	7.1	3.7	3.4	0.7	18	2.535211268	9.38028169	8.61971831	1.774647887
Radius4	7.1	3.2	5.5	0.9	10	1.408450704	4.507042254	7.746478873	1.267605634
Tibia1	8.5	5.5	6.2	2.1	12	1.411764706	7.764705882	8.752941176	2.964705882
Tibia2	11.3	4.7	8.7	1.3	17	1.504424779	7.07079646	13.08849558	1.955752212

Tibia3	13	4.9	10.3	1.2	25	1.923076923	9.423076923	19.80769231	2.307692308
Tibia4	12.5	3.3	9.9	0.8	16	1.28	4.224	12.672	1.024
Tibia5	11.4	4.6	5	1.4	16	1.403508772	6.456140351	7.01754386	1.964912281
Tibia6	12.8	6.5	4.8	1.9	22	1.71875	11.171875	8.25	3.265625
Ulna1	9.6	3.8	4.6	0.6	13	1.354166667	5.145833333	6.229166667	0.8125
Ulna2	11	2.9	9.6	0.9	26	2.363636364	6.854545455	22.69090909	2.127272727
Ulna3	6.3	3.1	5	0.5	18	2.857142857	8.857142857	14.28571429	1.428571429

	Incision L	Incision W	Bone L	Bone W
average	18.51724138	8.75007748	11.37394517	1.942835561
std dev	5.342689863	3.319535161	4.062818408	0.790394069
n	28			

Appendix B – Fixation Construct Analysis

Link to supplemental digital content:

https://docs.google.com/spreadsheets/d/1PYT9uhjF7J148YfpH9ZxR7MgD-YAyK8gWsQcRNRl4Nw/edit?usp=sharing

Appendix C – Exploratory Experiments

C.1 Overview

This section includes summary figures and data tables from the exploratory experiments with different sensor arrangements in different animal models.

C.2 Single parallel sensor measuring from tissue

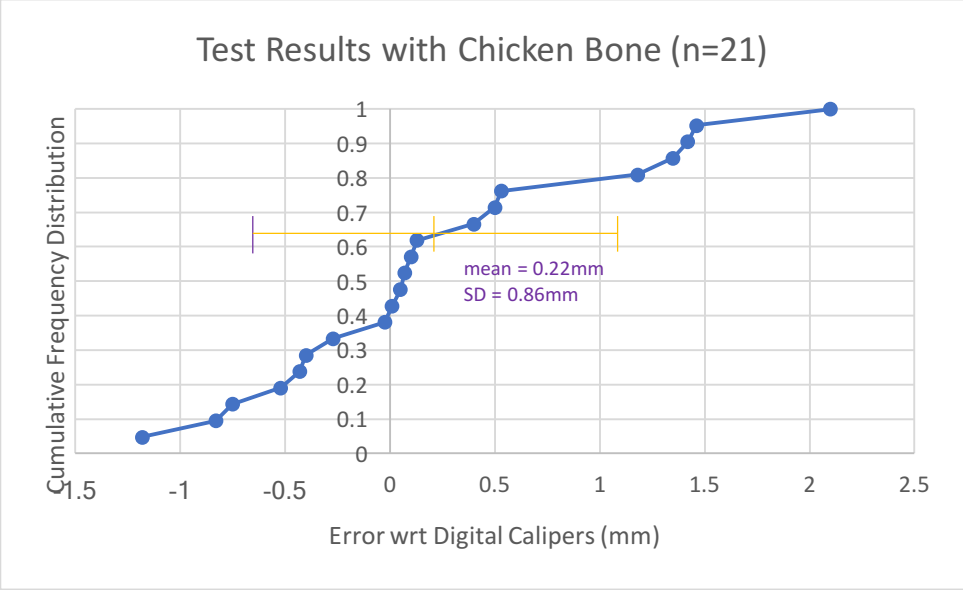

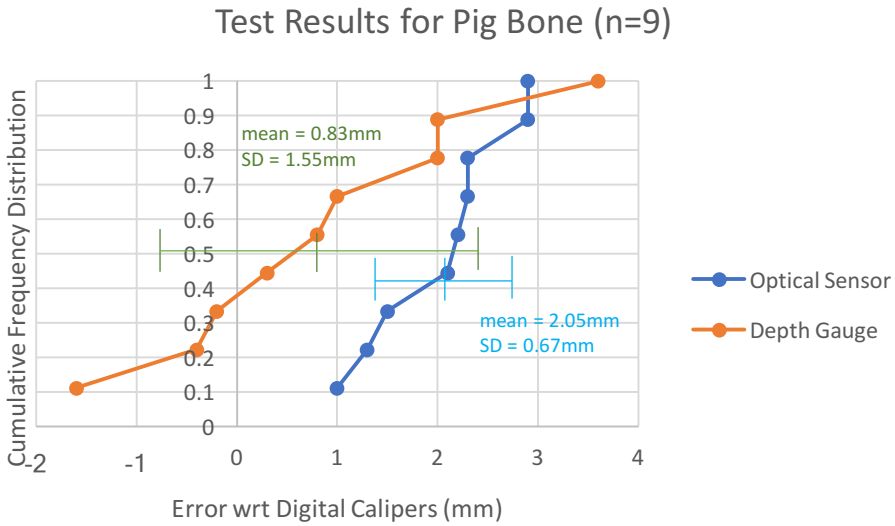

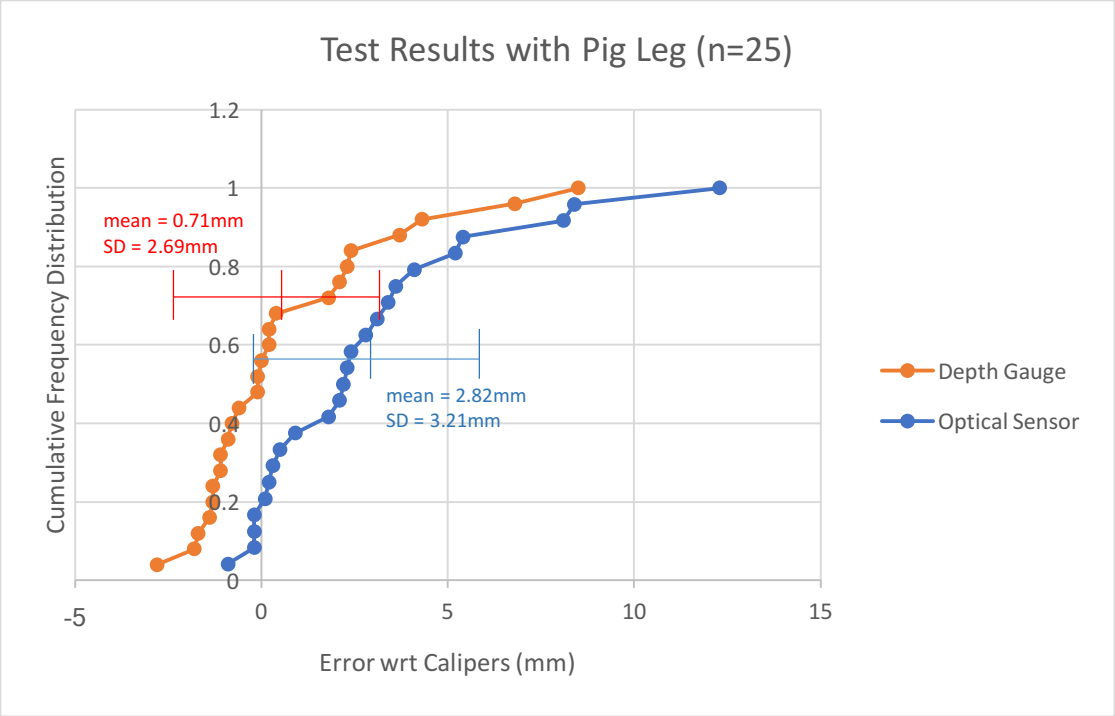
Test Results with Pig Leg (n=25)
Cumulative Frequency Distribution
1.2
1
0.8
0.6
0.4
0.2
0
-5
0
5
10
15
Error wrt Calipers (mm)
mean = 0.71mm
SD = 2.69mm
mean = 2.82mm
SD = 3.21mm
Depth Gauge
Optical Sensor

C.3 Paired parallel sensors measuring from tissue

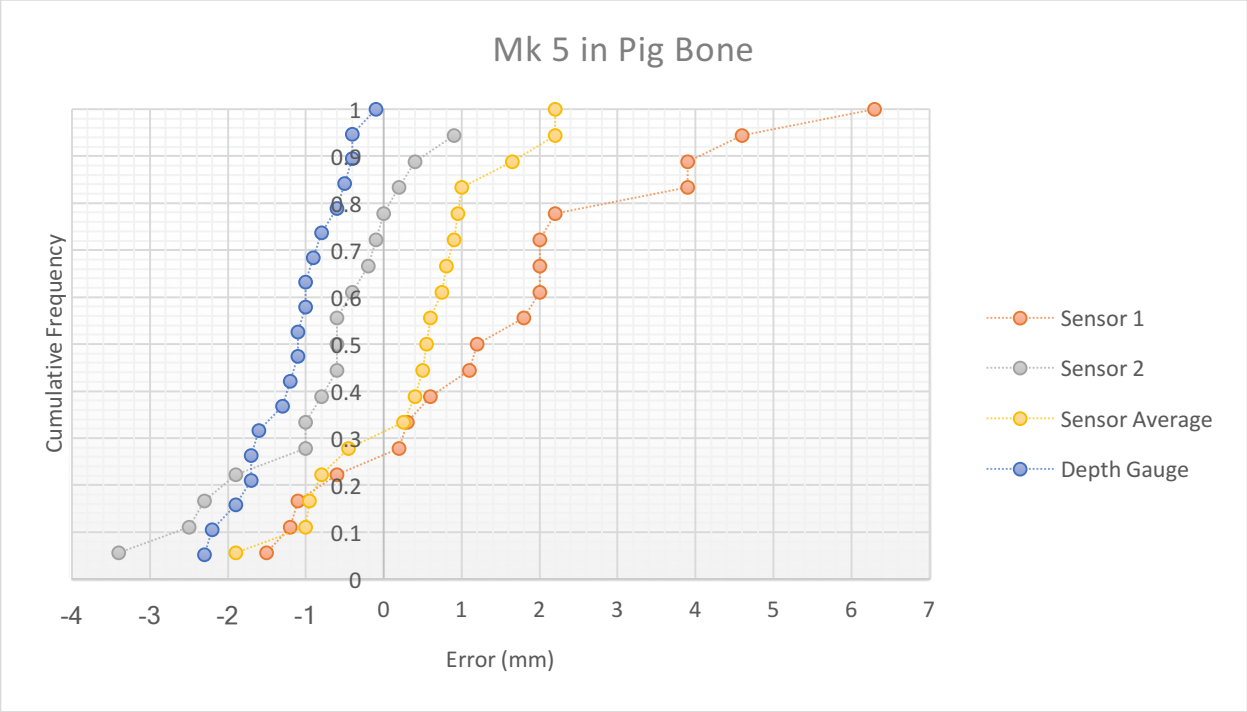

	Mean Error	Std Dev
Depth Gauge (n=19)	-1.15	0.62
Sensor 1 (n=18)	1.54	2.13
Sensor 2 (n=18)	-0.69	1.22
Sensor Average (n=18)	0.43	1.1

C.4 Paired angled sensors measuring from tissue

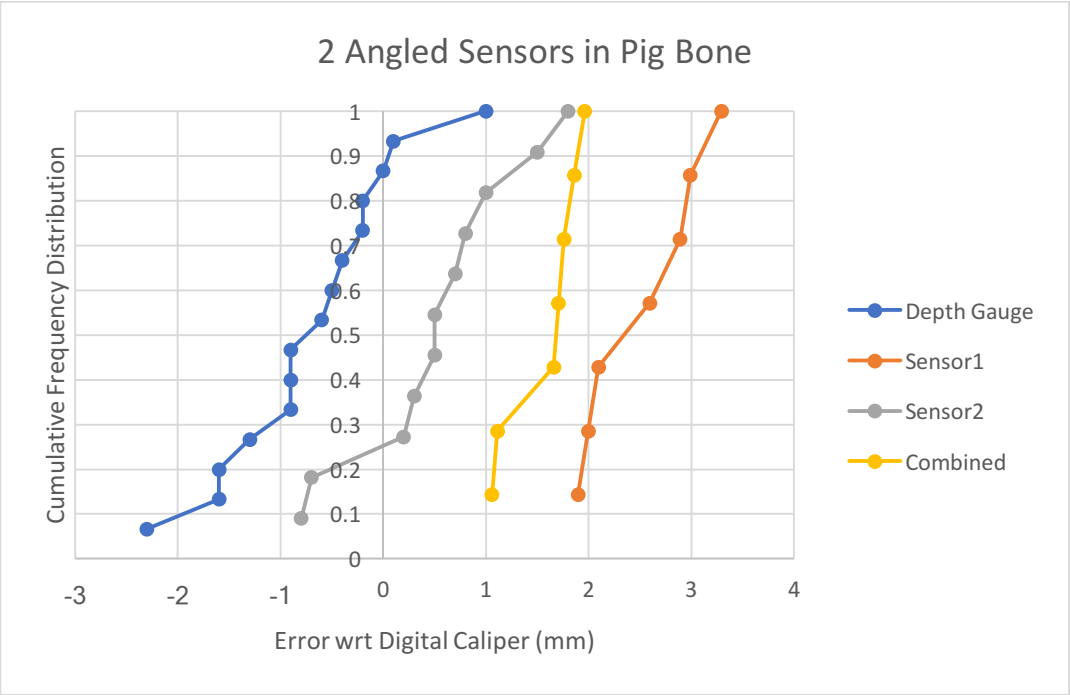

	Mean Error (mm)	SD (mm)
Depth Gauge (n=15)	-0.69	0.815
Sensor 1 (n=7)	2.79	0.7
Sensor 2 (n=11)	0.53	0.8
Combined (n=7)	1.59	0.36

C.5 Paired angled sensors measuring from drill guide

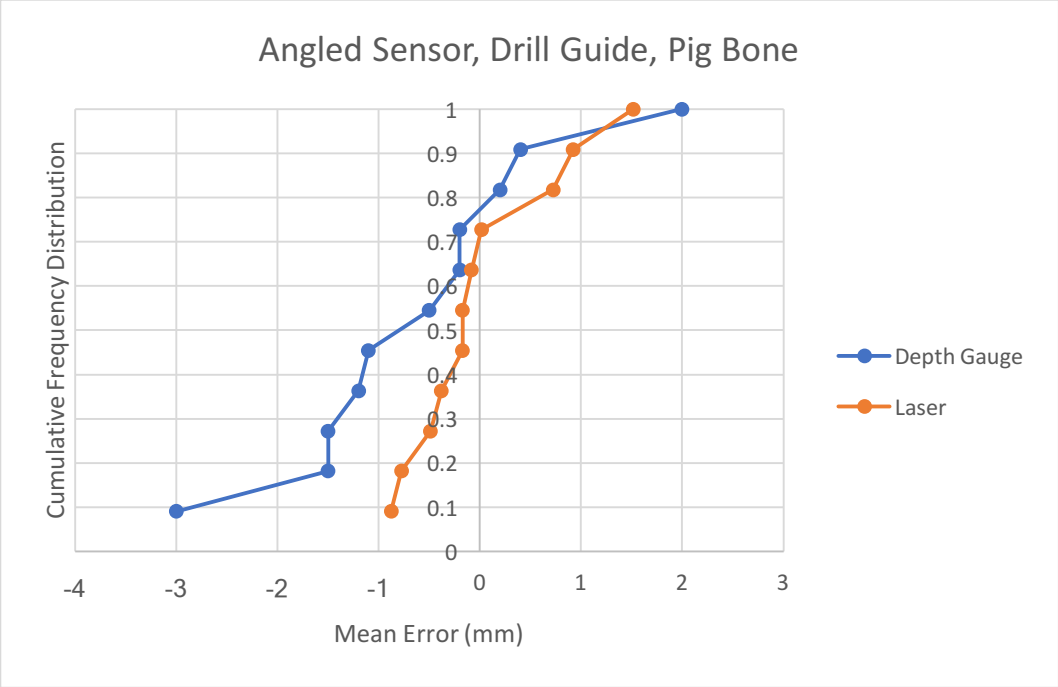

	Mean Error (mm)	SD (mm)
Depth Gauge	-0.6	1.29
Sensor 2	0.02	0.74

Appendix D – Final Evaluation Experiments

Link to supplemental digital content:

https://docs.google.com/spreadsheets/d/16ylK64joPV4DD9s1Sd_gsZgFF03ArgQOHMUZB-O5-oE/edit?usp=sharing

Appendix E – Sterilization Approval Process

E.1 Overview

The following information comes from an interview with Janet Bristair, Co-Ordinator of the Reprocessing Department Improvement Program at VGH. She would be involved in the process of bringing an experimental device into the OR.

E.2 Approval Process

Independent of the clinical research ethics process, a sterilization approval process needs to be followed prior to bringing a device into the operating room. The process is as involved for an experimental device as it would be for a commercial device. It requires contracting a third party laboratory to develop and validate a sterilization protocol for the device, as well as a detailed Standard Operating Procedure. The SOP and the certification of the sterilization protocol need to be provided to the reprocessing department of the hospital prior to the device being allowed into the OR.

For the laboratory I contacted (Alfamed Consulting, Winnipeg MB) three complete prototypes would be required to perform the validation studies. Estimated costs for the process are between $20 000 - $30 000. A timeline of approximately 3 months would also be needed.

E.3 Sterilization Methods

E.3.1 Autoclave Steam Sterilization

Method: Batch process with steam at 121^{o}C – 148^{o}C pressurized at 1-3.5 atm. These conditions kill all bacteria/viruses through protein denaturation etc (cooking)

Duration: 15-60 min

Indications: Most common/inexpensive sterilization process. Suitable for most surgical instruments. Temperatures above 125^{o}C can damage semiconductors, and will likely damage embedded batteries. Significant moisture involved, which could also damage components.

E.3.2 Ethylene Oxide (ETO) Sterilization

Method: Batch process with device/instruments placed in sealed container. Process involves five stages: evacuation and humidification, gas introduction, exposure, evacuation, and air washes. Max temp of 60^{o}C. ETO reacts with DNA, amino acids, and proteins to prevent microbial replication.

Duration: 8-12 hours

Indications: First method available for heat/moisture sensitive devices. Can work with semiconductors, but vacuum phase can affect embedded batteries

E.3.3 Chlorine Dioxide (CD) Gas Sterilization

Method: Batch process with device/instruments placed in sealed container. Process involves five stages: preconditioning with humidification, conditioning, generation and delivery of chlorine dioxide gas, exposure, and aeration). Max temp of 40^{o}C. Gas acts as an oxidizing agent, which damages cell membranes, and results in cell lysis and death.

Duration: 2.5 hours

Indications: Best process for devices that are temperature and moisture sensitive.

E.3.4 Vaporized Hydrogen Peroxide (VHP) Sterilization

Method: Batch process with three stages: conditioning including vacuum generation, H_2O_2 injection, and aeration. Max temp of 50°C. Mechanism is not completely understood, but involves production of reactive oxygen molecules.

Duration: 1.5 hours

Indications: Suitable for some moisture/temperature sensitive devices, however the vacuum can damage embedded batteries.

E.3.5 Hydrogen Peroxide Plasma Sterilization

Method: Batch process with four stages (vacuum generation, H_2O_2 injection, diffusion, and plasma discharge). Max temp of 65°C, with 13.56 MHz radiofrequency energy at 200 – 400W. Functions by free radical and reactive species generation by hydrogen peroxide gas and the plasma phase.

Duration: 1-3 hours

Indications: Similar low temperature/pressure/moisture as VHP, but also has less vacuum generation. However the high levels of RF energy can damage semiconductors in electronic components.

E.3.6 Gamma Ray Sterilization

Method: Continuous process where device is moved on a conveyor belt in proximity to cobalt 60, which emits radiation at between 1.17 MeV and 1.33 MeV. The radiation produces powerful oxidizing and reducing agents which result in degradation of essential cell components such as enzymes and DNA.

Duration: Variable

Indications: No temperature, moisture, or pressure associated damage with radiation sterilization. However the radiation degrades semiconductors, causing them to malfunction.

E.3.7 Electron Beam Sterilization

Methods: Continuous process where device is moved on a conveyor belt in proximity to an electron beam generator (similar to a cathode ray tube, but more powerful). Energy levels required for sterilization are between 5 -10 MeV. Radiation produces free radicals, which react with DNA and result in cell death.

Duration: Variable

Indications: Same as gamma, but does not produce/require nuclear materials. Electron beam will build up charge on electronic components and cause damage to semiconductors.